^{17}O nuclear-magnetic-resonance spectroscopic study of high-T_c superconductors

Eric Oldfield, Chris Coretsopoulos, Shengtian Yang, Linda Reven, Hee Cheon Lee, Jay Shore, Oc Hee Han, and Emannuel Ramli

School of Chemical Sciences, University of Illinois at Urbana–Champaign, 505 South Mathews Avenue, Urbana, Illinois 61801

and Materials Research Laboratory, University of Illinois at Urbana–Champaign, 104 South Goodwin Avenue, Urbana, Illinois 61801

David Hinks

Materials Science Division, Argonne National Laboratory, Argonne, Illinois 60439

(Received 27 March 1989)

We have obtained solid-state ^{17}O NMR spectra of a number of ^{17}O-enriched oxides and high-temperature oxide superconductors, including $Cu_2^{I}O$, $Cu^{II}O$, $KCu^{III}O_2$, Bi_2O_3, Tl_2O_3, $La_{1.85}Sr_{0.15}CuO_4$, $YBa_2Cu_3O_{7-x}$, $Bi_2Sr_2CaCu_2O_{8+x}$, $Tl_2Ba_2CaCu_2O_{8+x}$, and $Ba_{0.6}K_{0.4}BiO_3$. Spectra of all of the simple diamagnetic oxides contain relatively sharp resonances in a "diamagnetic" region of ~ -200 to $+700$ ppm (from H_2O, International Union of Pure and Applied Chemistry δ scale). $Cu^{II}O$ exhibits a broad resonance centered at ~ 4500 ppm. Spectra of all of the Cu-containing superconductors (at 300 K) contain a relatively broad and highly paramagnetically shifted peak, due to CuO_2 planes, at ≈ 1800 ppm, together with a peak or series of peaks, in a more normal diamagnetic region, $\approx 100-600$ ppm from H_2O. $YBa_2Cu_3O_{7-x}$ also contains a peak at ~ 2950 ppm, assigned to the chain [O(4)] sites. The highly shifted (CuO_2) features undergo a $\approx 1000-1300$ ppm diamagnetic shift in $YBa_2Cu_3O_{7-x}$ and $Tl_2Ba_2CaCu_2O_{8+x}$ upon cooling to 77 K ($< T_c$). These highly shifted features are absent in $Ba_{0.6}K_{0.4}BiO_3$, although the resonance in $Ba_{0.6}K_{0.4}BiO_3$ is ≈ 500 ppm paramagnetically shifted from that in the parent compound, $BaBiO_3$. ^{17}O NMR spectra of magnetically aligned samples of $YBa_2Cu_3O_{7-x}$ yield diagonal elements of the electric-field-gradient tensor (χ_{ii}) for the CuO_2 plane oxygens, O(2) and O(3), of $\pm(4.02, -6.46, 2.44)$ and $\pm(3.95, -6.51, 2.56)$ MHz. The observed resonance frequencies for both sites ($H_0 \| c$) are ≈ 1900 ppm from H_2O. For the CuO_2 plane in $Bi_2Sr_2CaCu_2O_{8+x}$ (at 300 K) and in $Tl_2Ba_2CaCu_2O_{8+x}$ (at 77 K) the quadrupole coupling constant (e^2qQ/h) is ≈ 6.4 MHz also. For the column or bridging oxygen [O(1)] in $YBa_2Cu_3O_{7-x}$, $e^2qQ/h \sim 7.3$ MHz and $\eta \approx 0$, at 300 K, the isotropic frequency shift is ~ 458 ppm, and the anisotropy of the chemical or Knight shift ($\Delta\sigma$) is ~ 657 ppm, with $\sigma_{\|} \| c$. A similar result is found for the apical oxygen in $La_{1.85}Sr_{0.15}CuO_4$, with $\sigma_{33} = \sigma_{\|} \sim 694$ ppm and $\sigma_{11} = \sigma_{22} = \sigma_{\perp} \sim 474$ ppm, determined on a magnetically ordered sample. For the chain site in $YBa_2Cu_3O_{7-x}$ [O(4)], we find $\chi_{ii} = \pm(3.38, -10.94, 7.56)$ MHz. Calculations suggest for all sites that V_{zz} is negative and is aligned along the Cu—O—Cu bond axis. Results on oxygen-depleted $YBa_2Cu_3O_{7-x}$ show considerable broadening of the plane-site features, consistent with the onset of antiferromagnetic ordering, while the column oxygens [O(1)] are much less affected. Temperature-dependence studies of T_1 for O(2,3) in $YBa_2Cu_3O_{7-x}$ indicate Korringa-type behavior above T_c, and the Knight shift predicted is in good accord with that observed. There is no BCS-type relaxation enhancement just below T_c. Overall, our results give a broad basis for the assignment of ^{17}O NMR resonances in most of the classes of high-temperature superconductors currently being investigated (2:1:4, 1:2:3, Bi_2Cu_2, Tl_2Cu_2, and Cu-free Bi-containing phases) and show considerable similarities in frequency shifts (and their temperature dependence), T_1, e^2qQ/h values, and spin-echo decay behavior, for the CuO_2 planes in each system, and between the (La(Sr)O,SrO,BaO) and (TlO,BiO) planes as well.

INTRODUCTION

While superconductivity in several metal oxides, including $SrTiO_3$ ($T_c \sim 0.3$ K),[1] Rb_xWO_3 ($T_c \sim 3$ K),[2] and $BaPb_{1-x}Bi_xO_3$ ($T_c \sim 13$ K),[3] has been known for a number of years, it was only with the investigation of Bednorz and Müller[4] (on the La-Ba-Cu-O system), that true "high-temperature" superconductivity was realized. As is now well known, their discovery was rapidly followed by the observation of superconductivity in the Y-Ba-Cu-O system at ~ 90 K,[5–7] followed about one year later by even higher T_c's in the Bi-Sr-Ca-Cu-O,[8,9] Tl-Ba-Cu-O, and Tl-Ba-Ca-Cu-O systems.[10] At present, although a number of mechanisms have been proposed to explain the high T_c's observed, none are yet fully accepted, and consequently considerable additional experimental and theoretical work on characterizing these novel materials is in progress worldwide.

One of the techniques currently in use is nuclear-magnetic-resonance (NMR) spectroscopy, which has a

long history of successful application in investigating the superconducting state, including early experimental verification of a central aspect of BCS theory.[11,12] NMR has also been applied recently to many of the nuclei in the high-T_c superconductors, including ^{63,65}Cu,[13–16] ^{89}Y,[17–19] and ^{139}La,[20,21] and has resulted in a number of interesting observations on band gaps, spectral assignments, Korringa relaxation, and so forth.

However, we feel that one of the most potentially informative nuclei, ^{17}O, remains to be investigated. The basis for our belief can be summarized as follows.

(1) All high-T_c superconductors are oxides, and are thus, in principle, amenable to NMR analysis.

(2) Cu-free materials having moderate T_c's have now been produced, and Cu NMR is obviously not applicable to these systems.

(3) There are always likely to be more nonequivalent oxygen sites than metal sites, so ^{17}O NMR can, again in principle, provide more structural probes than metal ion NMR.

(4) ^{17}O NMR (with labeled compounds) is easier than NMR of most metal ions present, due to its moderately good sensitivity due to a small quadrupole moment. Certainly, sensitivity (in powders) is much better than with copper, due to the very large quadrupole coupling constant values of copper.

Overall then, the idea behind our work is very simple: because all known high-T_c superconductors contain oxygen, because NMR spectroscopy has been a very useful technique to obtain information on structure and bonding (in diamagnetic materials, see, e.g., Ref. 22), and has also in the past been a powerful probe of superconductive behavior, we believe a comprehensive ^{17}O NMR investigation of a wide range of oxide superconductors is sure to yield a large body of interesting information about these new materials.

In this paper, we first give a brief theoretical background survey of some previous ^{17}O NMR studies of diamagnetic materials, outlining the chemical shift values found, the quadrupole coupling constants (e^2qQ/h), and relaxation behavior, then we discuss our results on high-T_c materials. We cover first the assignments for $YBa_2Cu_3O_{7-x}$, the most studied superconductor, then show results on the related $La_{1.85}Sr_{0.15}CuO_4$, $Bi_2Sr_2CaCu_2O_{8+x}$, and $Tl_2Ba_2CaCu_2O_{8+x}$ systems, together with, for comparison, results on the newer copper-free material $(Ba_{0.6}K_{0.4})BiO_3$. Results on the model compounds Cu_2O, $KCuO_2$, Bi_2O_3, and Tl_2O_3 are also included. Overall, our results suggest each Cu-containing phase contains a highly paramagnetically shifted oxygen (or oxygens), thought to reside in the CuO_2 planes, having very fast spin-lattice and spin-spin relaxation behavior. This feature is absent in the Cu-free system. The other planar sites in general have much more diamagnetically shifted resonances, in the "normal" range of a few hundred parts per million (ppm) upfield from $H_2{}^{17}O$, although the chain oxygen [O(4)] in $YBa_2Cu_3O_{7-x}$ is even more deshielded than any of the CuO_2 sites.

THEORETICAL BACKGROUND

Energy-level diagram and line shapes

We first show in Table I the relevant spin quantum number, abundance, relative sensitivity, and quadrupole moment data for ^{17}O, and for the two copper isotopes, ^{63}Cu and ^{65}Cu. At natural abundance, Cu NMR is clearly more sensitive than ^{17}O NMR, but with ^{17}O labeling, typical quadrupole coupling constants ($\approx$40–60 MHz for Cu, $\approx$5–10 MHz for ^{17}O) and the larger I value for oxygen, we find that ^{17}O NMR spectra can be quite rapidly obtained. This is very encouraging, since it implies—and we show—that ^{17}O NMR of all sites in most types of high-T_c material synthesized to date is feasible. This is an important point, since, for example, Cu NMR studies of the $La_{1.85}Sr_{0.15}CuO_4$, $Bi_2Sr_2CaCu_2O_{8+x}$, and $Tl_2Ba_2CaCu_2O_{8+x}$ phases has to date proven rather difficult, due to extremely broad spectral linewidths. In contrast, ^{17}O NMR of, e.g., $Tl_2Ba_2CaCu_2O_{8-x}$ yields three peaks, due to the CuO_2, BaO, and TlO planar sites (see below). Spectral assignments can be made by comparison between a range of high-T_c materials, and various model compounds (such as Tl_2O_3).

The major line-broadening effect in ^{17}O NMR is in general the quadrupole interaction, for which we find the following Hamiltonian, H:

$$H=-\gamma\hbar HI+\frac{e^2qQ}{4I(2I-1)}[3I_z^2-I(I+1)+\tfrac{1}{2}\eta(I_+^2+I_-^2)], \quad (1)$$

which yields the following energies:

$$E=-\gamma\hbar Hm+\frac{e^2qQ}{4I(2I-1)}\left[\frac{3\cos^2\theta-1}{2}\right][3m^2-I(I+1)]-\frac{3(e^2qQ)^2}{16h(\gamma H/2\pi)I^2(2I-1)^2}m\{\tfrac{3}{2}\cos^2\theta(1-\cos^2\theta)[8m^2-4I(I+1)+1]+\tfrac{3}{8}(1-\cos^2\theta)^2[-2m^2+2I(I+1)-1]\}. \quad (2)$$

TABLE I. NMR parameters for copper and oxygen.

Nucleus	Spin	Natural abundance (%)	Relative sensitivity	Quadrupole moment (10^{-24} cm^2)
^{17}O	$\frac{5}{2}$	3.7×10^{-2}	2.91×10^{-2}	-2.6×10^{-2}
^{63}Cu	$\frac{3}{2}$	69.1	9.31×10^{-2}	-0.16
^{65}Cu	$\frac{3}{2}$	30.9	0.114	-0.15

We show in Fig. 1(a) the Zeeman and first-order quadrupole interactions for an $I=\frac{5}{2}$ nucleus. For a single crystal, or oriented microcrystalline array, we would obtain a spectrum much as in Fig. 1(b). In a continuous wave (or selective-excitation field or frequency-sweep experiment), the peak intensities would be $\pm\frac{5}{2}\leftrightarrow\frac{3}{2}$, $\frac{5}{35}$; $\pm\frac{3}{2}\leftrightarrow\pm\frac{1}{2}$, $\frac{8}{35}$; and $\frac{1}{2}\leftrightarrow-\frac{1}{2}$, $\frac{9}{35}$. However, for a random, polycrystalline material, the line shape is that of the powder average shown in Fig. 1(c). Fortunately, we can determine e^2qQ/h from the overall spectral breadth, and the isotropic chemical shift (δ_i) is essentially that of the (unbroadened) central ($\frac{1}{2}\leftrightarrow\frac{1}{2}$) transition. When e^2qQ/h is small, magic-angle sample spinning is successful in yielding improved spectral resolution and signal-to-noise ratios. Both e^2qQ/h and δ_i can be readily measured from such spectra.[23]

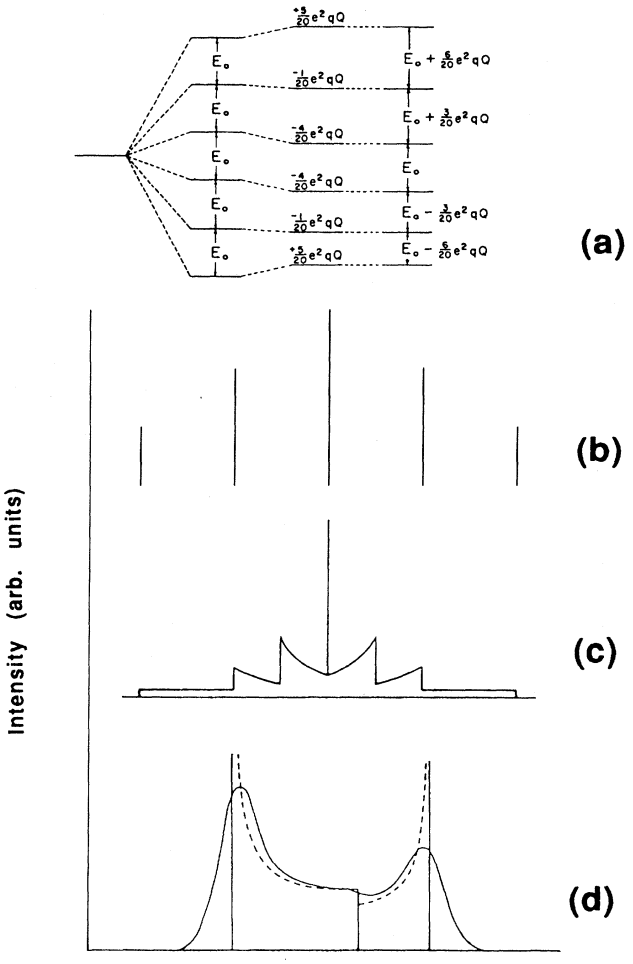

FIG. 1. Theoretical energy-level diagram and line shapes for $I=\frac{5}{2}$. (a) Energy-level diagram showing the Zeeman and first-order quadrupole interactions. (b) Line spectrum for a single crystal or oriented powder, oriented at $\theta=0$. (c) Powder pattern. (d) Line-shape function (dashed line) and symmetrically broadened line shape (solid line) for the central transition ($m=\frac{1}{2}\leftrightarrow-\frac{1}{2}$) when second-order quadrupole effects are dominant, and $\eta=0$.

When e^2qQ/h is a sizable fraction of the Larmor frequency ω_0 then second-order quadrupole effects begin to be noticeable, and the central transition undergoes further broadening, and we show in Fig. 1(d) a typical theoretical second-order powder pattern of the $\frac{1}{2}$-$\frac{1}{2}$ transition (for an axially symmetric electric field gradient, efg, tensor). Such spectra are typically found with, for example, the Si-O-Si oxygens in SiO_2, or in the zeolite ZSM-5,[24] and we show below such line shapes for the Ba-O and Tl-O sites in $Tl_2Ba_2CaCu_2O_{8+x}$. Computer simulation of such experimental line shapes yields both e^2qQ/h, the asymmetry parameter (η) of the electric-field-gradient tenor, and the isotropic chemical (or frequency) shift δ_i. In general, it is desirable to measure such second-order powder patterns at two magnetic field strengths, to confirm the nature of the line broadening, as we show below for $Tl_2Ba_2CaCu_2O_{8+x}$.

Coupling constants and chemical shifts

Since there have been so few ^{17}O NMR studies of solids reported to date, we will first give a brief overview of the ^{17}O NMR e^2qQ/h values and chemical shifts found in simple diamagnetic compounds, which are germane to any discussion of the ^{17}O NMR behavior of high-T_c materials. Figure 2 gives a convenient graphical compilation of the e^2qQ/h values found for a wide range of oxides, plotted as a function of the ionic character of the bonds in hypothetical fragments, *A*-O-*B*.[25] As can be seen, the highly ionic materials have small e^2qQ/h values, while the more covalent systems (e.g., *C*-O-*C*)

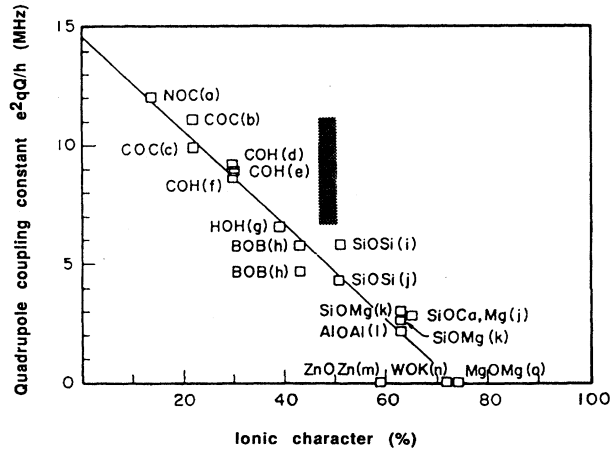

FIG. 2. Plot of ^{17}O nuclear quadrupole coupling constant (e^2qQ/h, MHz) vs average percent ionic character for a series of *A*-O-*B* fragments, where *A* and *B* are cations. The experimental e^2qQ/h values are for a series of oxides or simple oxyanions. The percent ionic character is the arithmetic mean of the single-bond values obtained from the Pauling electronegativities of elements *A*, *B*, and O. Compounds used were as follows: (a) *N*-methylsyndone, (b) tetrahydropyran, (c) xanthene, (d) tetrachlorohydroquinone, (e) 2,5-dichlorohydroquinone, *N*-methylsyndone, (f) *p*-chlorophenol, (g) normal hexagonal ice, (h) B_2O_3, (i) low cristobalite, (j) diopside, (k) forsterite, (l) Al_2O_3, (m) zinc oxide, (n) potassium tungstate, (o) magnesium oxide. The hatched area represents the range of e^2qQ/h values found in $YBa_2Cu_3O_{7-x}$.

have much larger values. Such a correlation is of course wholly empirical, and totally ignores symmetry effects. Nevertheless, it appears to have widespread utility as a predictor of e^2qQ/h values. More detailed approaches to calculations of e^2qQ/h values in oxides, having similar ionicities, can be found elsewhere.[22,26]

If we use the results of Fig. 2 to predict the e^2qQ/h values for oxygen in the Cu-O-Cu fragments in high-T_c materials, we find from the relation[25]

$$|e^2qQ/h|(\text{MHz}) = -0.203I(\%) + 14.8 , \quad (3)$$

where I is the % ionic character of the Cu—O—Cu bond, that $e^2qQ/h \sim 5.3$ MHz (using Pauling electronegativities of 3.5 for O, 1.9 for Cu, the Cu—O is 47% ionic). This is close to the value we find experimentally for the CuO_2 planes in $YBa_2Cu_3O_{7-x}$, $Bi_2Sr_2CaCuO_{8+x}$, and $Tl_2Ba_2CaCu_2O_{8+x}$, and the Cu-O-Cu column oxygen in $YBa_2Cu_2O_{7-x}$, but is much less than that of the chain oxygen in $YBa_2Cu_3O_{7-x}$ (see below). The region encompassing our results with Cu—O—Cu bonds in high-T_c systems is shown in Fig. 2 by the hatched area. We show below that somewhat better agreement with experiment can be obtained by using a theoretical relationship proposed previously for linear, or close to linear, A—O—B bonds.[22]

Some generalization about the range of ^{17}O chemical shifts can be made from the data shown in Table II. First, these results indicate that the chemical shifts of

TABLE II. Solid-state ^{17}O NMR chemical shifts in oxides and oxyanions.[a]

Compound	Chemical shift (δ_i, ppm)	Ref.	Compound	Chemical shift (δ_i, ppm)	Ref.
H_2O	0	IUPAC ($\delta=0$)	Pr_6O_{11}	2150	This work
BeO	26	b	SiO_2	46	This work
MgO	47	b	SnO (black)	247	c
CaO	294	b	SnO_2	105	c
SrO	390	b	PbO (red)	289	c
BaO	629	b	TiO_2	591	c
BaO_2	334	This work	CeO_2	877	This work
ZnO	−18	b			
CdO	46–141	b	$CaMgSi_2O_6$	63,69,84	d
HgO	121	b	α-$CaSiO_3$	75,91,94	d
$Zn_4O(dtp)_6$[e]	−49	f	α-$SrSiO_3$	80,105,108	d
Al_2O_3	72–79	g	$BaSiO_3$	87,159,169	d
In_2O_3	97	c	SiOSi (zeolites)	~44–52	h
Tl_2O_3	364	This work	SiOAl (zeolites)	~31–40	h
Bi_2O_3	196	This work	SiOGa (zeolites)	~29	i
$BaBiO_3$	375	This work			
Sc_2O_3	355	c	AlOP($AlPO_4$-n)	~61–63	i
Y_2O_3	356	This work			
La_2O_3	≈500	c, this work	K_2WO_4	422,429,437	f
Eu_2O_3	−3212	This work	$KMnO_4$	1197	f
$Cu_2^{I}O$	−181	This work			
$Cu^{II}O$	≈4500	This work	MO_2 (IrO_2, PtO_2 compounds)	~325–385	j
$KCu^{III}O_2$	≈30	This work	Picket fence porphyrin (FeO_2)	2020,1600	k

[a]All results were obtained in this laboratory using isotopically enriched materials at 8.45 and/or 11.7 T by means of static spin-echo-computer simulations and/or magic-angle sample-spinning techniques. All chemical shifts are in ppm from H_2O with high-field, low-frequency, paramagnetic or deshielded values being designated as positive (International Union of Pure and Applied Chemistry δ scale).

[b]Reference 23.

[c]Data courtesy of Dr. G. L. Turner (unpublished results).

[d]H. K. C. Timken, S. E. Schramm, R. J. Kirkpatrick, and E. Oldfield, J. Phys. Chem. **91**, 1054 (1987).

[e]dtp≡diisopropylphosphorodithioato.

[f]Reference 25.

[g]T. H. Walter and E. Oldfield (unpublished results).

[h]H. K. C. Timken, G. L. Turner, J.-P. Gilson, L. B. Welsh, and E. Oldfield, J. Am. Chem. Soc. **108**, 7231 (1986).

[i]Reference 26.

[j]H. C. Lee and E. Oldfield, J. Magn. Res. **69**, 367 (1986).

[k]H. C. Lee. C. Coretsopoulos, and E. Oldfield (unpublished results). Also, H. C. Lee, Ph.D. thesis, University of Illinois at Urbana, 1988 (unpublished).

most diamagnetic oxides will be in the range $-200-+700$ ppm from H_2O [where high-frequency, low-field, paramagnetic, or deshielded values are positive, International Union of Pure and Applied Chemistry (IUPAC) δ scale]. The extremes of the range are BaO (629 ppm) and Cu_2O (-181 ppm). Diamagnetic species resonating outside this range include oxoanions, where single oxygen atoms are multiply bonded to a single metal site (such as $KMnO_4$), together with exotics such as FeO_2 complexes (picket-fence porphyrins, hemoglobin, and myoglobin)—all of which contain complex covalent bonding arrangements, involving multiple (π) bonds.

To date, we have only investigated three paramagnetic oxides: CuO, Eu_2O_3, and Pr_6O_{11}. At room temperature, all spectra are very broad and highly shifted. While not wishing to digress, we note that the ^{17}O NMR spectrum of CuO is characterized by a rapid spin-echo decay time constant (T_{2e}) and does not average under magic-angle sample spinning (MASS)—as we find later with the high-T_c materials, while that of Eu_2O_3 decays much more slowly and does average under MASS, resulting in large numbers of narrow spinning sidebands (data not shown). These observations could well originate from exchange interactions in CuO, while much of the broadening in Eu_2O_3 may be due to the low-lying J states (see Ref. 27 for a recent discussion of MASS NMR in paramagnetic solids). In any case, these results, together with those on the diamagnetic solids, give us an initial benchmark data set of (largely unpublished) ^{17}O NMR chemical shifts with which to compare results to be described on the high-temperature superconductors.

EXPERIMENTAL ASPECTS

Nuclear magnetic resonance spectroscopy. ^{17}O NMR spectra were obtained on Fourier-transform (FT) NMR spectrometers operating at 67.8 and 48.8 MHz, using Oxford Instruments (Osney Mead, Oxford, U.K.) 11.7-T, 52-mm bore or 8.45-T, 89-mm bore superconducting solenoid magnets. We used Nicolet Instrument Corporation (Madison, WI) Model-1180 and Model-1280 computer systems for data acquisition, and Amplifier Research (Souderton, PA) Model-200L and -150LA and Henry Radio (Los Angeles, CA) Model-2002 amplifiers for final rf pulse generation. Static ^{17}O spectra were obtained using "home-built" horizontal solenoid-type sample probes. ^{17}O 90° pulse widths on H_2O were typically ~ 6 μsec. Chemical shifts are reported in ppm from external standards of tap water, using the δ scale. Most spectra were recorded using a spin-echo technique.[28] Where appropriate, samples were magnetically ordered as described previously.[29,30] Digital resolution in the latter spectra was 30 ppm.

Synthetic aspects. All samples were synthesized using conventional solid-state routes from oxides or oxide-carbonate mixtures, basically as described previously for $YBa_2Cu_3O_{7-x}$.[29] Oxygen-deficient $YBa_2Cu_3O_{7-x}$ samples (where $x=1.0$, 0.7, and 0.3) were prepared by heating separately at 600 °C portions from an ^{17}O-enriched mother batch ($x=0.1$) and subjecting these portions to a dynamic vacuum for different periods of time. The $x \approx 0.5$ sample was prepared by heating appropriate amounts of CuO, BaO, and Y_2O_3 in an argon atmosphere at 950 K, and contained trace amounts of Y_2BaCuO_5 and $BaCuO_2$ impurities. It was ^{17}O labeled at 500 °C in a static $^{17}O_2$ atmosphere. Values of x were estimated by comparison with published x-ray diffraction results.[6] $Bi_2Sr_2CaCu_2O_8$ was prepared from Bi_2O_3 (Aldrich, Milwaukee, WI), $SrCO_3$, $CaCO_3$, CuO (Aesar, Seabrook, NH) at 4:3:3:4 composition. The finely ground mixture was initially fired in air at 850 °C for 4 h, then at 860 °C for 5 h, pressed into pellet form, then refired at 860 °C for 12 h. Powder x-ray analysis indicated a monophasic material identical with published data on $Bi_2Sr_2CaCu_2O_8$.[9] Labeling with ^{17}O was achieved by evacuating the sample for 3 h, followed by annealing in a static 35–50% $^{17}O_2$ (Monsanto Research Corporation, Miamisburg, OH) atmosphere at 500 °C for 45 h. Powder x-ray analysis of such ^{17}O-enriched samples were identical to those of the unenriched material. Unlabeled $Tl_2Ba_2CaCu_2O_8$ was prepared from Tl_2O_3 (Johnson Matthey) and $Ba_2Ca_2Cu_3O_7$ (prepared from $BaCO_3$, $CaCO_3$, and CuO at 2:2:3 mole ratio). The finely ground mixture was pressed into pellet form, wrapped with gold foil, then heated at 890 °C for 15 min under an $^{16}O_2$ flow. The sample was then air cooled. Powder x-ray analyses showed a monophasic material, identical with published data on $Tl_2Ba_2CaCu_2O_8$.[10] Labeling of $Tl_2Ba_2CaCu_2O_8$ was basically the same as with $Bi_2Sr_2CaCu_2O_8$. We also made a sample of $Tl_2Ba_2CaCu_2O_{8+x}$ from ^{17}O-enriched Tl_2O_3 and ^{17}O-enriched $Ba_2Ca_2Cu_3O_7$, basically as described above for the initial ^{16}O sample of $Tl_2Ba_2CaCu_3O_{8+x}$. $La_{1.85}Sr_{0.15}CuO_4$ and $(Ba_xK_{1-x})BiO_3$ systems were prepared using standard methods.[31,32] The purity of all phases was verified by powder x-ray diffraction (using a Rigaku D/Max diffractometer). T_c onsets were determined with a S.H.E. (San Diego, CA) superconducting quantum interference magnetometer. All T_c onsets were as expected, although the transition breaths varied somewhat, due in part, perhaps, to our use of very fine powders for the NMR experiments. We were unable to detect any significant impurities by x-ray diffraction (even in epoxy-embedded samples), except as mentioned below for the $Tl_2{}^{17}O_3/Ba_2Ca_2Cu_3{}^{17}O_7$ material.

RESULTS AND DISCUSSION

General summary of bases for ^{17}O NMR spectral assignments. Previous work on the Cu NMR and nuclear quadrupole resonance (NQR) of $YBa_2Cu_3O_{7-x}$ and $YBa_2Cu_3O_6$ has shown that the assignment of even one or two peaks can be a difficult matter, so that the assignment of even more peaks, as found with ^{17}O NMR, is likely to be even more complex, and the well-known difficulties associated with isotopic labeling could further complicate matters.[33,34] However, with enough structures, *prediction* of NMR behavior should become possible, which hopefully should result in assignment verifications. Correct assignments then pave the way for more interesting studies of site-dependent relaxation, and frequency shifts, as a function of temperature.

Before detailing our results on each of the high-T_c phases we have investigated, we first summarize the types of information we have used to make such assignments,

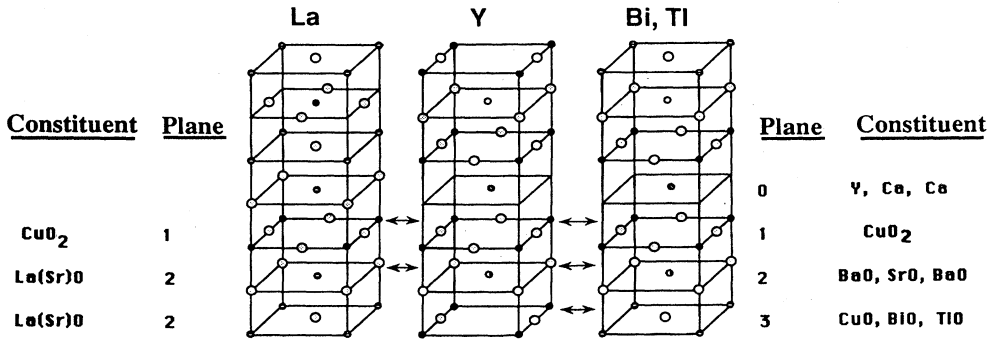

FIG. 3. Schematic diagram showing partial structures of $La_{1.85}Sr_{0.15}CuO_4$ (left), $YBa_2Cu_3O_{7-x}$ (center), and $Bi_2Sr_2CaCu_2O_{8+x}$ (Bi) and $Tl_2Ba_2CaCu_2O_{8+x}$ (Tl) (right). Similarities between planes 1 and 2 in the La(Sr) and Y, Bi, Tl systems are indicated (↔).

then we discuss the detailed assignments of all oxygens in $YBa_2Cu_3O_{7-x}$, compare these results with the La(Sr), Bi_2Cu_2, and Tl_2Cu_2 phases, and finally survey the $(Ba,K)BiO_3$ system. The general basis for our assignments is as follows.

(1) All Cu-containing superconductors contain a broad, highly paramagnetically shifted peak, at $\approx$1800 ppm from H_2O.

(2) This feature is absent in the Cu-free system, and might thus reasonably be assigned to a common structural feature, the CuO_2 planes.

(3) This feature is the most intense one in the $YBa_2Cu_3O_{7-x}$ system.

(4) This feature undergoes a large ($\sim$0.15%) diamagnetic shift on cooling below T_c, in $YBa_2Cu_3O_{7-x}$, and in $Tl_2Ba_2CaCu_2O_{8+x}$, consistent with a decrease in the spin susceptibility contribution to the Knight shift.

(5) Four pairs of approximately equal intensity satellites are observed for this highly shifted feature, in $YBa_2Cu_3O_{7-x}$, consistent with a planar CuO_2 [O(2), O(3)] assignment.

(6) Spin-lattice and spin-spin relaxation times in the CuO_2 planes are much faster than in the non-CuO_2 planar sites (which have more normal, diamagnetic shifts).

(7) Rotation patterns for the axial, bridging BaO oxygen [O(1)] in magnetically oriented $YBa_2Cu_3O_{7-x}$ yields assignment of the BaO planar (bridging) oxygen in $YBa_2Cu_3O_{7-x}$. The peak resonates in the normal "diamagnetic" shift region. Similar behavior is found for the axial site in $La_{1.85}Sr_{0.15}CuO_4$.

(8) Satellite transitions for this peak in $YBa_2Cu_3O_{7-x}$ are consistent with a close to axially symmetric efg.

(9) The chain oxygen [O(4)] in $YBa_2Cu_3O_{7-x}$ is also highly shifted, consistent with local moments on Cu(1), but is apparently absent in spectra of the Bi_2Cu_2 and Tl_2Cu_2 system.

(10) The other planar sites (2 and 3) in the Bi_2Cu_2 and Tl_2Cu_2 systems are close in shift (but not identical to) those of the parent oxides (SrO, BaO, Bi_2O_3, Tl_2O_3).

$YBa_2Cu_3O_{7-x}$—SPECTRAL ASSIGNMENTS

We show in Fig. 3 the structure of the high-temperature superconductor $YBa_2Cu_3O_{7-x}$. To facilitate comparison between results on $YBa_2Cu_3O_{7-x}$ with those on the other superconductors, we have arbitrarily assigned four *plane designations* (planes 0–3), as shown in Fig. 3. Y^{3+} is alone in plane 0; O(2), and O(3) are in the CuO_2 plane, plane 1; the Cu(1)-O(1) bridging oxygen [O(1)] is in the BaO plane, plane 2; plane 3 contains the chain oxygen, O(4). Also shown in Fig. 3 is the (partial) structure of $La_{1.85}Sr_{0.15}CuO_4$, drawn to emphasize its similarities with $YBa_2Cu_3O_{7-x}$. The Bi_2Cu_2 and Tl_2Cu_2 species also have very similar structures to $YBa_2Cu_3O_{7-x}$, as indicated in Fig. 3.

We show in Fig. 4 the 48.8-MHz (8.45-T) ^{17}O NMR spectra of a powder sample of $YBa_2Cu_3{}^{17}O_{7-x}$ at 300 and at 77 K, Figs. 4(a) and 4(b). There are clearly two main features in the 300 K spectrum: an intense peak at $\sim$1800 ppm and a weaker set of peaks at $\approx$300 ppm. On cooling into the superconducting state, Fig. 4(b), the intense feature undergoes a diamagnetic shift of $\sim$800 ppm, while the less intense feature remains at approximately the same chemical shift. Taken together, we believe these intensity and shift results lead to a tentative

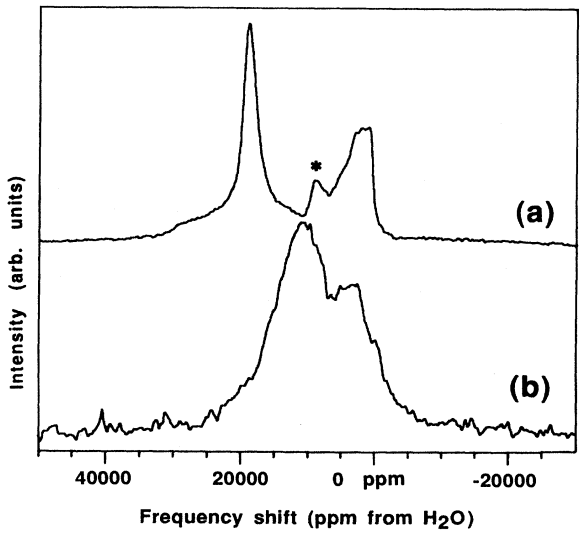

FIG. 4. 8.45-T (48.8-MHz) ^{17}O spin-echo spectra of random powder sample of $YBa_2Cu_3O_{7-x}$ at (a) 300 K and (b) 77 K. The * indicates a resonance from O(1) in aligned crystallites.

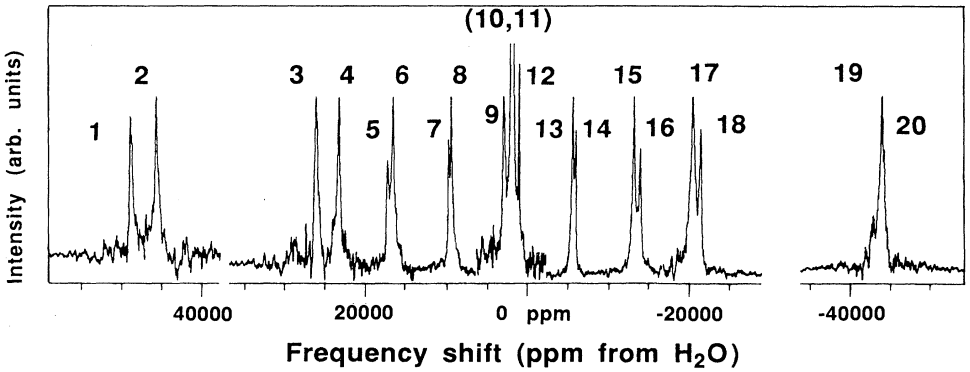

FIG. 5. 8.45-T (48.8-MHz) ^{17}O NMR spectra of magnetically aligned $YBa_2Cu_3O_{7-x}$ ($H_0 \| c$), at 300 K. The peak intensities have been equalized for clarity. The actual intensities for central and satellite transitions have the appropriate 9:8:5 relative intensity ratios. 19 of the possible 20 transitions (four oxygens × five transitions) can be observed; the central transitions for O(2,3) overlap. Connectivities for the individual sites are as follows: O(1), peaks 2, 4, 12, 18, 19; O(2,3), peaks 5–8, (10,11), 13–16; O(4), peaks 1, 3, 9, 17, 20.

assignment of the intense feature to the plane sites [four oxygens, O(2) and O(3)], while the weaker feature, which shifts much less with temperature, Fig. 4(b), can be assigned to the column site [two oxygens, O(1)]. We show later that the chain oxygen [one oxygen, O(4)] resonates at ~3000 ppm, and has a very large (~100 kHz) second-order breadth, and is thus broadened beyond detection limits, in powder samples. Results on a Eu^{3+}-substituted material, which tend to confirm the CuO_2 plane assignment, have been presented elsewhere.[29]

In order to obtain enhanced resolution, we have investigated magnetically ordered samples, and a composite spectrum is shown in Fig. 5. The resolution is remarkably increased over that of the powder spectrum, and reveals a total of 19 peaks for the five transitions of the four nonequivalent oxygen sites. Only the $(\frac{1}{2}\leftrightarrow-\frac{1}{2})$ transition for the planar oxygens [O(2,3)] is unsplit.

The results of Fig. 5 indicate that four pairs of satellite transitions (peaks 5–8, 13–16) of the central ~1900-ppm feature (peak 10+11) can be readily resolved. The overall intensity, intensity ratios, and ≈1:1 splitting of each feature strongly supports our assignment of the ≈1800-ppm central transition feature (in the powder sample) to the CuO_2 (plane 1) oxygens O(2) and O(3), which might reasonably be expected to have slightly different e^2qQ/h values (permitting resolution in the satellite regions). The intensity ratio of the $\pm\frac{5}{2}\leftrightarrow\pm\frac{3}{2}$ to $\pm\frac{3}{2}\leftrightarrow\pm\frac{1}{2}$ transitions (1:1.18) is in reasonable agreement with that expected (1:1.16).

From second-order perturbation theory we find

$$\nu(\tfrac{5}{2}\leftrightarrow\tfrac{3}{2})=\nu_0+\tfrac{3}{10}\chi_{zz}-\frac{(\chi_{xx}-\chi_{yy})^2}{400\nu_0}\ , \tag{4}$$

$$\nu(\tfrac{3}{2}\leftrightarrow\tfrac{1}{2})=\nu_0+\tfrac{3}{20}\chi_{zz}+\frac{(\chi_{xx}-\chi_{yy})^2}{320\nu_0}\ , \tag{5}$$

$$\nu(\tfrac{1}{2}\leftrightarrow-\tfrac{1}{2})=\nu_0+\frac{(\chi_{xx}-\chi_{yy})^2}{200\nu_0}\ , \tag{6}$$

$$\nu(-\tfrac{1}{2}\leftrightarrow-\tfrac{3}{2})=\nu_0-\tfrac{3}{20}\chi_{zz}+\frac{(\chi_{xx}-\chi_{yy})^2}{320\nu_0}\ , \tag{7}$$

$$\nu(-\tfrac{3}{2}\leftrightarrow-\tfrac{5}{2})=\nu_0-\tfrac{3}{10}\chi_{zz}-\frac{(\chi_{xx}-\chi_{yy})^2}{400\nu_0}\ , \tag{8}$$

where $\chi_{\alpha\alpha}=eQV_\alpha/h$ are the Cartesian components of the electric-field-gradient tensor, and ν_0 is the center of the resonance. The z axis is defined along the crystallographic c axis.

Adding Eqs. (5) and (7), and (4) and (8), we find

$$\nu(\tfrac{3}{2}\leftrightarrow\tfrac{1}{2})+\nu(-\tfrac{1}{2}\leftrightarrow-\tfrac{3}{2})=2\nu_0+\frac{(\chi_{xx}-\chi_{yy})^2}{160\nu_0} \tag{9}$$

and

$$\nu(\tfrac{5}{2}\leftrightarrow\tfrac{3}{2})+\nu(-\tfrac{3}{2}\leftrightarrow-\tfrac{5}{2})=2\nu_0-\frac{(\chi_{xx}-\chi_{yy})^2}{200\nu_0} \tag{10}$$

and subtracting Eqs. (9) and (10), and (5) and (7), we find

$$[\nu(\tfrac{3}{2}\leftrightarrow\tfrac{1}{2})+\nu(-\tfrac{1}{2}\leftrightarrow-\tfrac{3}{2})]-[\nu(\tfrac{5}{2}\leftrightarrow\tfrac{3}{2})+\nu(-\tfrac{3}{2}\leftrightarrow-\tfrac{5}{2})]=\frac{9(\chi_{xx}-\chi_{yy})^2}{800\nu_0} \tag{11}$$

and

$$\nu(\tfrac{3}{2}\leftrightarrow\tfrac{1}{2})-\nu(-\tfrac{1}{2}\leftrightarrow-\tfrac{3}{2})=\tfrac{3}{10}\chi_{zz}\ . \tag{12}$$

Since $\chi_{xx}+\chi_{yy}+\chi_{zz}=0$, we can solve for χ_{xx}, χ_{yy}, and χ_{zz}. Table III shows the observed and predicted shifts on two different samples, sample I at both 8.45 and 11.7 T (data not shown), and sample II (Fig. 5) at 8.45 T. We find the following averaged diagonal elements of the efg tensor for the plane sites: $(\chi_{xx},\chi_{yy},\chi_{zz})=\pm(3.95,-6.51,2.56)$ MHz and $\pm(4.02,-6.46,2.44)$ MHz. There is excellent agreement between observed and predicted shifts, Table III. Given the expected experimental errors, this result implies an e^2qQ/h value of ~6.5 MHz, with near axial symmetry ($\eta\sim0.2$–0.25) about an axis perpendicular to the c axis. The χ_{ii} results given above are about 10% higher than those reported previously, due to use of a better oriented sample, obser-

vation of more transitions, and an alternate method of calculation (not involving measurement of the field dependence of the frequency shift of the central transition).

We can also detect the central and satellite transitions for the column oxygen O(1) in Fig. 5 (peaks 2, 4, 12, 18, and 19). The satellite separations indicate close to axial symmetry. We previously recorded ^{17}O NMR spectra (at 8.45 and 11.7 T) on another magnetically ordered sample, as a function of rotation about an axis perpendicular to the ordering (c) axis.[29] For the plane sites, we found complex powder patterns were generated as the sample was rotated about the a-b plane. However, for any axially symmetric site whose principal electric-field-gradient tensor axis (V_{zz}) and chemical (or Knight) shift tensor axis (δ_{zz}) is aligned *along* c, a sharp line is expected, as a function of rotation angle, in agreement with our experimental observation. The expression for the chemical shift as a function of rotation angle θ for such an oriented array rotated about an axis perpendicular to the principal axis is

$$\delta(\theta)=\delta_i+\frac{\Delta\delta}{3}(3\cos^2\theta-1)-\frac{9}{800}\left[\frac{e^2qQ}{\nu_0 h}\right]^2(1-\cos^2\theta)\times(9\cos^2\theta-1)\times 10^6 , \quad (13)$$

where δ_i is the isotropic shift, $\Delta\delta=\delta_\perp-\delta_\parallel$ is the chemical (or Knight) shift anisotropy, and e^2qQ/h is the quadrupole coupling constant. We previously determined that, for the column (or bridging) oxygen O(1), $\delta_i=458$ ppm, $\Delta\delta=657$ ppm, $e^2qQ/h=7.7$ MHz, and $\eta=0$. Since our previous results also strongly support close to axial symmetry, we now estimate that the diagonal elements of the efg tensor are $\approx\pm(3.65,3.65,-7.29)$ MHz, in reasonable agreement with our previous result using the sample rotation technique, of $e^2qQ/h\sim 7.7$ MHz.

Using our previous observation that the isotropic shift $\delta_i=458$ ppm, we can estimate the 0° ($H_0\|c$) shift for the column site to be $458+\frac{2}{3}(657)=896$ ppm. Experimentally, we find $\delta=924$ ppm, in very good agreement with the previous result. The calculated result from the satellite transitions is 931 ppm. Thus both the sample rotation and satellite transition observations are in good agreement.

The remaining peaks in Fig. 5 (peaks 1, 3, 9, 17, 20) must then originate from the chain site, O(4). Using the same approach as outlined above, we find good agreement between observed and calculated frequency shifts, as shown in Table IV. For O(4), we find $\chi_{ii}=\pm(3.38,-10.94,7.56)$ MHz, or $e^2qQ/h=10.9$ MHz and $\eta\sim 0.38$.

Using the Townes-Dailey approach described previously,[22] and the expected ~47% ionic character of the Cu—O—Cu bonds which can be deduced from the Paul-

TABLE III. Experimental and theoretical frequency shifts of planar oxygens in magnetically aligned $YBa_2Cu_3{}^{17}O_{7-x}$ at 8.45 and 11.7 T and derived diagonal elements of electric-field-gradient tensor.

	Transition	ν(obs), ppm[a]	ν(calc), ppm[a]	ν(obs), ppm[b]	ν(calc), ppm[b]	ν(obs), ppm[c]	ν(calc), ppm[c]
Site A[d]	$\frac{5}{2}\leftrightarrow\frac{3}{2}$	17 220	17 271	17 237	17 224	12 967	12 965
	$\frac{3}{2}\leftrightarrow\frac{1}{2}$	9688	9663	9660	9660	7425	7426
	$\frac{1}{2}\leftrightarrow-\frac{1}{2}$	1890	1883	1914	1913	1813	1803
	$-\frac{1}{2}\leftrightarrow-\frac{3}{2}$	−6093	−6067	−6008	−6016	−3901	−3902
	$-\frac{3}{2}\leftrightarrow-\frac{5}{2}$	−14 139	−14 189	−14 132	−14 130	−9696	−9693
Site B[e]	$\frac{5}{2}\leftrightarrow\frac{3}{2}$	16 619	16 604	16 564	16 601	12 476	12 474
	$\frac{3}{2}\leftrightarrow\frac{1}{2}$	9372	9378	9362	9375	7216	7218
	$\frac{1}{2}\leftrightarrow-\frac{1}{2}$	1890	1973	1914	1959	1813	1873
	$-\frac{1}{2}\leftrightarrow-\frac{3}{2}$	−5604	−5612	−5610	−5625	−3559	−3560
	$-\frac{3}{2}\leftrightarrow-\frac{5}{2}$	−13 389	−13 376	−13 319	−13 379	−9084	−9082
		Diagonal elements of electric-field-gradient tensor (χ_{ii}, MHz)					
Site A[d]		$\pm(3.94,-6.50,2.56)$[a]		$\pm(4.11,-6.66,2.55)$[b]		$\pm(3.80,-6.36,2.56)$[c]	
Site B[e]		$\pm(4.12,-6.56,2.44)$[a]		$\pm(3.96,-6.40,2.44)$[b]		$\pm(3.98,-6.42,2.44)$[c]	
		Average diagonal elements of electric-field-gradient tensor (χ_{ii}, MHz)					
Site A[d]				$\pm(3.95,-6.51,2.56)$			
Site B[e]				$\pm(4.02,-6.46,2.44)$			

[a]8.45 T, sample I.
[b]8.45 T, sample II.
[c]11.7 T, sample I.
[d]Site characterized by larger $e^2/qQ/h$ value.
[e]Site characterized by smaller e^2qQ/h value. These sites correspond to O(2) and O(3), but cannot be assigned on a 1:1 basis, so have been called A and B.

TABLE IV. Experimental and theoretical frequency shifts of chain oxygen O(4) in magnetically aligned $YBa_2Cu_3O_{7-x}$ at 8.45 T and derived diagonal elements of electric-field-gradient tensor (χ_{ii}).

Transition	Frequency shift (ppm) ν(obs)	ν(calc)
$\frac{5}{2}\leftrightarrow\frac{3}{2}$	48 838	48 801
$\frac{3}{2}\leftrightarrow\frac{1}{2}$	26 025	26 048
$\frac{1}{2}\leftrightarrow-\frac{1}{2}$	2953	2971
$-\frac{1}{2}\leftrightarrow-\frac{3}{2}$	−20 409	−20 428
$-\frac{3}{2}\leftrightarrow-\frac{5}{2}$	−44 149	−44 149
Diagonal elements of electric-field-gradient tensor (χ_{ii}, MHz)		
O(4)	±(3.38, −10.94, 7.56)	

ing electronegativities [ε(O)=3.5, ε(Cu)=1.9], we deduce for a 165° Cu—O—Cu bond that $e^2Qq_{xx}=e^2Qq_{yy}=+5.5$ MHz and $e^2Qq_{zz}=-11$ MHz. Although we are unable to assign the χ_{ii} values to the crystallographic axes, the above calculation certainly suggests that V_{zz} is negative and directed along the Cu—O—Cu bond axis. Addition of a partial O hole in the σ bonding orbital increases e^2qQ/h.

We can also draw some conclusions about the chemical shift or Knight shift anisotropy of the planar oxygens O(2,3) from our results on powder and oriented samples. We find that the overall breadth of the O(2,3) resonance is about 1300 ppm, at both 8.45 and 11.7 T, strongly indicating a close to axially symmetric chemical or Knight shift tensor, with $\sigma_{11}=\sigma_{22}=\sigma_{\perp}\sim1800$ ppm, and $\sigma_{33}=\sigma_{\parallel}\sim3100$ ppm. In a sample oriented at 0° ($H_0\|c$) we find the resonance for O(2,3) to be at ~1800–1900 ppm, while in a sample rotated 90° about c, we generate a powder pattern, with a σ_{33} edge at ~3100 ppm.[29] Since we do not observe a well-behaved rotation pattern for O(2,3) like that observed for the column of bridging oxygen, we conclude that the chemical or Knight shift tensor elements must be $\sigma_{xx}=1800$ ppm, $\sigma_{yy}=1800$ ppm, and $\sigma_{zz}=3100$ ppm. We cannot specifically identify the frequency shifts as Knight shifts, since solely orbital effects in conventional diamagnetic insulators such as K_2WO_4, $Mo(CO)_6$, and oxypicket fence porphyrin, are all in the same general range, ~500–2000 ppm. However, given the metallic nature of the CuO_2 planes, the demonstration of Korringa relaxation, and the identification of the overall shift as a Knight shift (see below), identification of the shift anisotropy as primarily a Knight shift anisotropy seems very plausible. Given also that the most deshielded element of the shift tensor for the bridging oxygen, O(1), is along the Cu—O—Cu bond direction, it is also possible that δ_{33} (and V_{zz} for the plane sites) are also oriented along the Cu—O—Cu bond axis.

Previously, we assigned O(1), O(2), and O(3) as above.[29] We also quoted the work of Bleier *et al.*,[35] and stated we had reproduced their observation of a peak at ~200–300 ppm, which they assigned to O(4). However, estimates of the intensity of this feature, the fact that it does not narrow significantly on magnetic ordering [in fact, it contains a major O(1) component], our observation of a ~3000-ppm feature in our oriented sample, Hammel's observation of the $\pm\frac{1}{2}\leftrightarrow\pm\frac{3}{2}$ transitions for O(4) in their sample,[36] and our own observation of 19 of the 20 possible transitions in a magnetically aligned sample of $YBa_2Cu_3O_{7-x}$, when taken together indicate that O(4) does in fact resonate even further downfield from the plane sites, but appears to be undetectable in powder samples. The 200–300-ppm features could arise from broken chains, or perhaps $C^{17}O_3^{2-}$ (at ~194 ppm).

The enhanced breadth and large apparent shift for O(4) we have observed could well correlate with the presence of antiferromagnetic spin fluctuations in the CuO chains, much as we have observed in the antiferromagnet CuO itself (see below).

We show in Fig. 6 ^{17}O NMR spectra of oxygen-depleted powder samples of $YBa_2Cu_3O_{7-x}$, and in Figs. 6 and 7 we show ^{17}O NMR results on such materials as a function of temperature. There is a slight high-field shift of the CuO_2 plane-site resonance on going from $O_{6.95}$ to $O_{6.5}$, with, apparently, a major broadening on further oxygen loss. This result is consistent with the very large

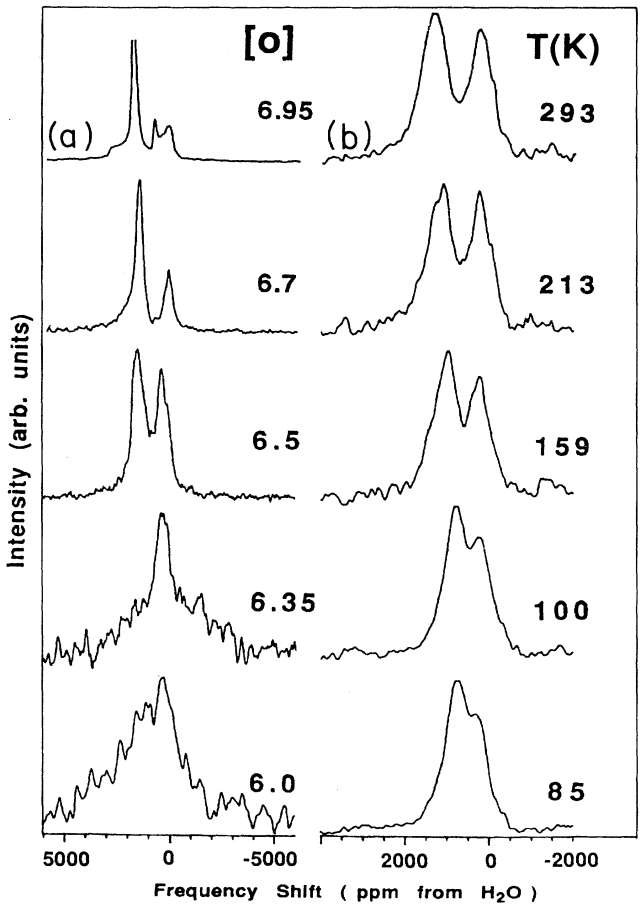

FIG. 6. 8.45-T (48.8-MHz) ^{17}O NMR spectra of (a) $YBa_2Cu_3O_{7-x}$ as a function of oxygen content at 300 K, (b) $YBa_2Cu_3O_{6.5}$ spectra, as a function of temperature.

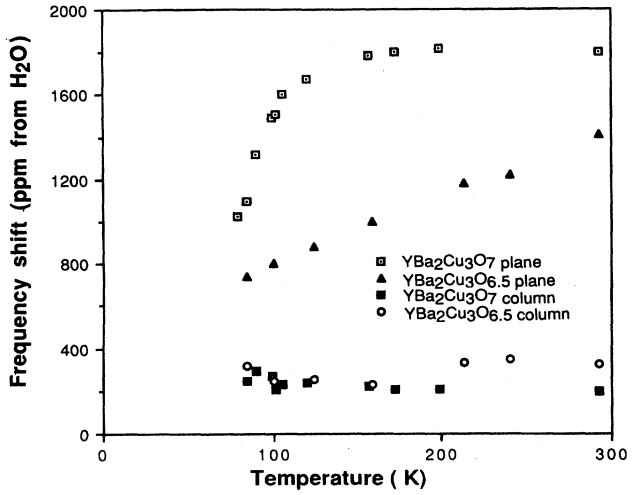

FIG. 7. 8.45-T (48.8-MHz) ^{17}O NMR frequency shifts as a function of temperature for the plane and column oxygen sites $YBa_2Cu_3O_{7-x}$ and $YBa_2Cu_3O_{6.5}$.

linewidth observed in the paramagnet-antiferromagnet CuO, and taken together with the temperature-dependence results on the $O_{6.5}$ species (Figs. 6 and 7) suggests the onset of strong antiferromagnetic interactions in species with O levels $\lesssim 6.5$.[37] As can be seen from Figs. 6 and 7, the column oxygens are relatively unaffected, at least down to O level ~ 6.50, and possibly down to O levels ~ 6.35.

We believe these results are generally supportive of the assignments to O(1) and O(2,3) given above. Thus the planar oxygen site resonance is about twice as intense as that of the bridging oxygen site resonance, and its resonance frequency has the largest temperature dependence. There are no clear indications (in powder samples) of O(4), which would be consistent with a location in the ~ 3000-ppm region, its very large second-order breadth (~ 100 kHz), and the fact that it is primarily O(4) which is removed upon oxygen depletion. Although preliminary, our results show no evidence for any major increase in T_1 on oxygen depletion, at least down to $O_{6.5}$, for O(1–3).

COMPARISONS WITH OTHER HIGH-T_c MATERIALS AND OTHER OXIDES

If the results and assignments we have presented above are correct, then it seems reasonable to make a number of predictions about the ^{17}O NMR behavior of other high-T_c materials. It seems reasonable to suppose that highly shifted peaks, due to CuO_2 planes, might be present in all Cu-containing materials, and if these large shifts are due, at least in part, to the presence of Cu(II) ions, then they would likely be absent in Cu-free systems. In addition, we might expect numerous features in the diamagnetic region (say -200–700 ppm), due to BaO, SrO, BiO, TlO, LaO, etc. planes, in the appropriate compositions.

To facilitate discussion, we refer back to Fig. 3 in which we presented a schematic diagram of the structures of four of the five materials of interest: $La_{1.85}Sr_{0.15}CuO_4$, $YBa_2Cu_3O_{7-x}$, $Bi_2Sr_2CaCu_2O_{8+x}$, and $Tl_2Ba_2CaCu_2O_{8+x}$. Figure 8 presents the ^{17}O NMR spectra of each material, obtained using a spin-echo method, at 11.7 T and 300 K.

Clearly, each of the Cu-containing systems has an extremely broad and highly shifted feature at ≈ 1800 ppm from H_2O (the actual width and peak maximum cannot be accurately determined from a single spectrum, but the maxima are close to those apparent), together with a much narrower feature or series of features in the region ≈ 0–600 ppm from H_2O (diamagnetic region). The highly shifted feature is absent in the Cu-free sample. These results can all be qualitatively explained on the assumption that the highly shifted features are due to oxygen

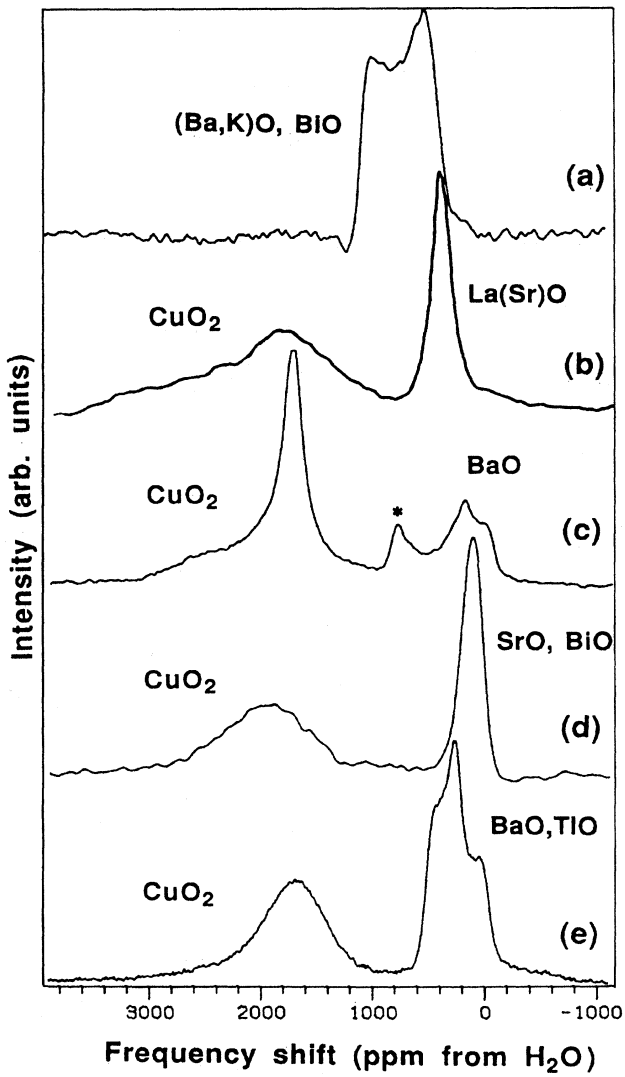

FIG. 8. 11.7-T (67.8-MHz) ^{17}O NMR spectra at 300 K of (a) $(Ba_{0.6}K_{0.4})BiO_3$, (b) $La_{1.85}Sr_{0.15}CuO_4$, (c) $YBa_2Cu_3O_{7-x}$, (d) $Bi_2Sr_2CaCu_2O_{8+x}$, and (e) $Tl_2Ba_2CaCu_2O_{8+x}$. The * in (c) represents O(1) sites in a small population of aligned crystallites (which also contribute to the 1800-ppm feature).

atoms in the CuO_2 planes, and that magnetic hyperfine interactions are a primary cause of the large shifts. Since the linewidths are so broad, they cannot arise solely from quadrupole interactions (since e^2qQ/h values are known) or to dipolar interactions with Cu or ^{17}O. They are not T_1 dominated (see below), and hence must contain major contributions from anisotropic chemical and/or Knight shifts, from exchange coupling, or from some sort of heterogeneous distribution of shifts. This latter possibility appears not to be the case for $YBa_2Cu_3O_{7-x}$, as determined from the magnetic alignment experiments.

In sharp contrast to these shifted and/or broad features, each Cu-containing sample has a narrower feature (or features) in the "diamagnetic" region of the spectrum. It is very tempting to assign each of these features to planes 2 and 3, in which case they could arise as follows:

$La_{1.85}Sr_{0.15}CuO_4$	(La,Sr,)O (plane 2)
$YBa_2Cu_3O_{7-x}$	BaO (plane 2)
$Bi_2Sr_2CaCu_2O_{8+x}$	SrO (plane 2)
	BiO (plane 3)
$Tl_2Ba_2CaCu_2O_{8+x}$	BaO (plane 2)
	TlO (plane 3)

We already assigned the $\delta = \sim 458$-ppm peak in $YBa_2Cu_3O_{7-x}$ to the BaO plane [plane 2, column oxygen O(1)]. Now, while it may be premature to make large numbers of additional assignments, given the difficulties expected to be associated with synthesis and ^{17}O labeling of some phases, we shall nevertheless discuss the results we have obtained, since we do predict a number of peaks in the high-field region, which is what is actually found. For example, with $Tl_2Ba_2CaCu_2O_{8+x}$, as shown in Figs. 8 and 9, there are clearly two sites present in the high-field region, having the following e^2qQ/h, η, and δ_i parameters, as determined from computer simulations of the 8.45- and 11.7-T ^{17}O NMR spectra, Fig. 9:

$$e^2qQ/h = \begin{cases} 8.8 \text{ MHz}, & \eta = 0.13, \quad \delta_i = 315 \text{ ppm} \\ 5.35 \text{ MHz}, & \eta = 0.30, \quad \delta_i = 350 \text{ ppm} \end{cases}$$

for sites *A* and *B*, respectively. We have obtained good agreement between 8.45- and 11.7-T spectra and simulations using the above parameters, with a $\sim 1{:}1$ intensity distribution. We believe this is suggestive of our observing the BaO (plane 2) and TlO (plane 3) oxygens, which should have a 1:1 intensity ratio—confirming our idea that isotopic labeling can be quite uniform. However, we caution that synthesis of pure ^{17}O-labeled Tl and Bi phases is expected to be rather difficult, and there is the ever present danger of selective labeling of minor impurity phases (which could be amorphous or otherwise difficult to detect by x-ray methods) when gas phase

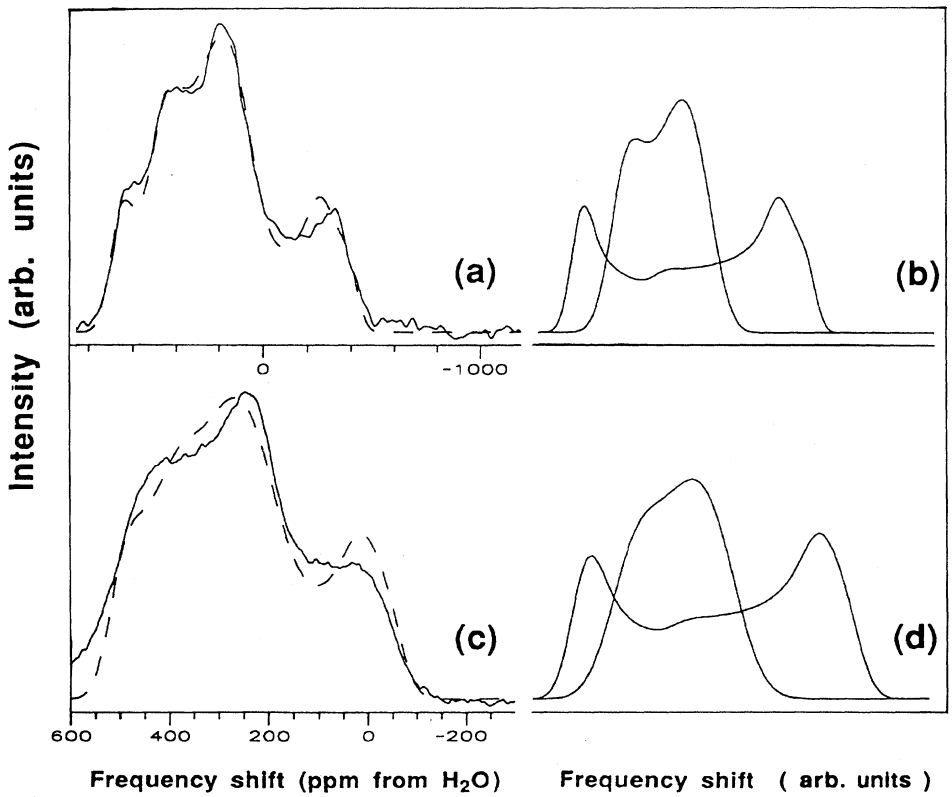

FIG. 9. ^{17}O NMR spectra (left) at 8.45 T (top) and 11.7 T (bottom) and computer simulations (right) of TlO and BaO sites in $Tl_2Ba_2CaCu_2O_{8+x}$, at 300 K. Fitting parameters were $\delta_i = 315$ ppm, $e^2qQ/h = 8.8$ MHz, $\eta = 0.13$, and $\delta_i = 350$ ppm, $e^2qQ/h = 5.35$ MHz, $\eta = 0.30$.

routes are involved. For $Tl_2Ba_2CaCu_2O_{8+x}$, we thus used in addition a synthesis from ^{17}O-enriched Tl_2O_3 and ^{17}O-enriched $Ca_2Ba_2Cu_3{}^{17}O_7$, and found again a major peak at ~243 ppm (the same shift as the major singularity in the gas phase exchanged material), and broader, less intense features at ~1600 ppm *and* ~2500 ppm. This sample showed good flux exclusion, but contained detectable impurities by XRD. Nevertheless, since neither starting material had features at these resonance shifts, these results do support the tentative assignments given above, as does the large diamagnetic shift of the ~1700-ppm features on cooling to 77 K (see below).

If these ideas are correct, then we would also expect to see two peaks in the diamagnetic region of $Bi_2Sr_2CaCu_2O_{8+x}$. Figure 8 gives little evidence for this. However, one- and two-dimensional spin-nutation experiments, as well as saturating comb-recovery experiments (data not shown), both suggest two components, having δ_{iso}~280, 197 ppm, but their similarities in T_1 and e^2qQ/h warrant further verification of this conclusion.

For $La_{1.85}Sr_{0.15}CuO_4$, the results of Fig. 8 indicate a single peak in the diamagnetic region, having δ_i~480 ppm. There appear to be no additional peaks in a nutation spectrum (data not shown). We have also been able to obtain ^{17}O NMR spectra of magnetically aligned $La_{1.85}Sr_{0.15}CuO_4$, as shown in Fig. 10(a). We find little evidence for sharp satellite transitions for the plane oxygens, as found with $YBa_2Cu_3O_{7-x}$, implying that the satellites must be rather broad, a result paralleling the broad Cu NMR linewidths found in this system, perhaps by coincidence. We also find that the sharp [La(Sr)O] resonance remains quite sharp on sample rotation, and its resonance shift as a function of rotation angle (θ) maps out a $3\cos^2\theta-1$ pattern, as shown in Fig. 10(b). Because of this, we assign this feature to the apical oxygens, aligned along the crystallographic c axis. We find the frequency-shift tensor to be axially symmetric, with $\sigma_{11}=\sigma_{22}=\sigma_\perp=481$ ppm, and $\sigma_{33}=\sigma_\parallel=715$ ppm. This behavior explains the observation (at both 8.45 and 11.7 T) of an apparent isotropic shift of ~480 ppm, which corresponds to observation of the dominant $\sigma_\perp$ edge of a powder pattern, at ~480 ppm. There is also a pronounced orientation dependence to the width of this line, which we believe corresponds with our observation in the $YBa_2Cu_2O_{7-x}$ system (see below) of a rapid T_{2e} behavior for the column or bridging oxygen [O(1)] for $H_0\|c$, and much longer T_{2e} behavior for $H_0\perp c$ (the $\sigma_\perp$ edge dominates the spectrum of the random powder). From the rotation pattern of $La_{1.85}Sr_{0.15}CuO_4$, we deduce an isotropic shift, δ_i ~559 ppm. The observation that the rotation pattern is described by a simple $P_2(\cos\theta)$ dependence implies that second-order quadrupole effects are small, i.e., e^2qQ/h is very small [unlike in $YBa_2Cu_2O_{7-x}$, where O(1) is some 7.3 MHz]. This is consistent with our results on the pulse width nutation behavior found for the

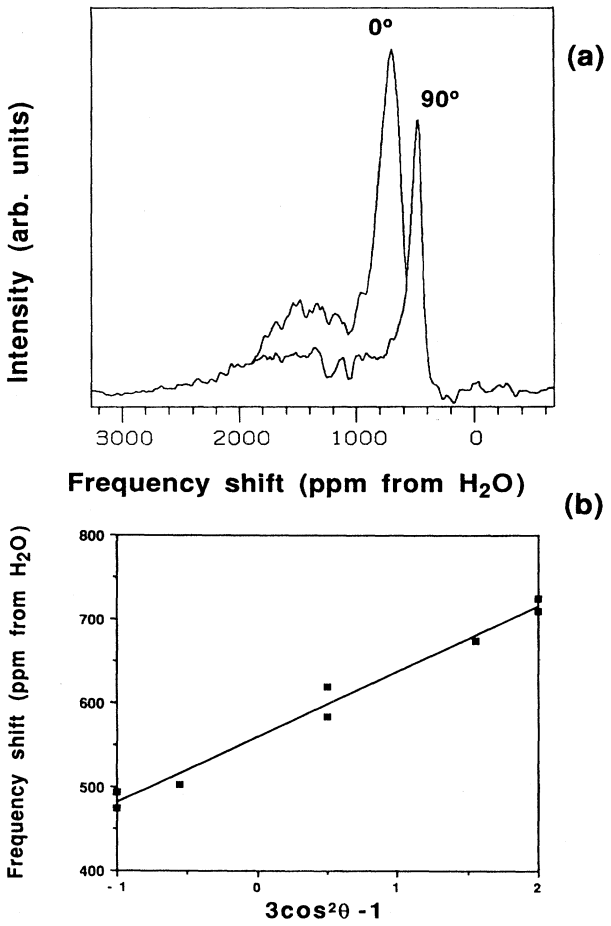

FIG. 10. 8.45-T (48.8-MHz) ^{17}O NMR results on magnetically aligned $La_{1.85}Sr_{0.15}CuO_4$. (b) Graph showing frequency shift of the peak maximum as a function of $(3\cos^2\theta-1)$, where θ is the rotation angle in degrees ($0°=H_0\|c$).

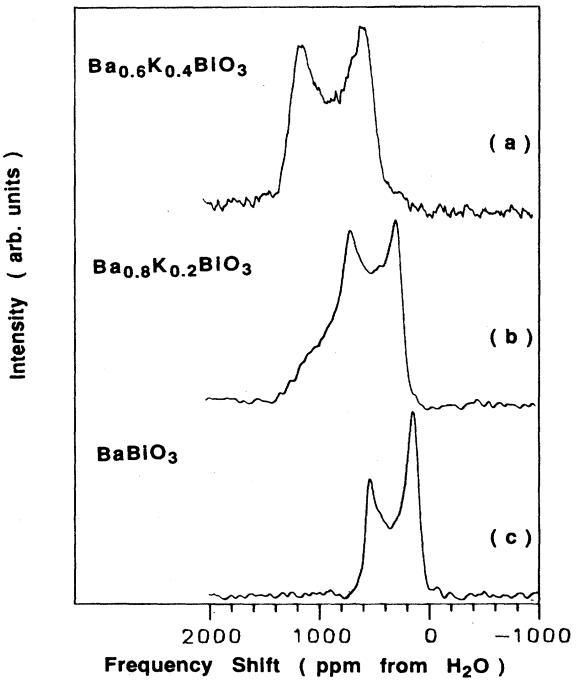

FIG. 11. 11.7-T (67.8-MHz) ^{17}O NMR spectra at 300 K of oxides in the (Ba,K)BiO_3 system. (a) $Ba_{0.6}K_{0.4}BiO_3$. (b) $Ba_{0.8}K_{0.2}BiO_3$. (c) $BaBiO_3$.

apical oxygen in $La_{1.85}Sr_{0.15}CuO_4$, where we find a maximum in signal intensity for a 3–4-μsec pulse width, where H_2O has a maximum intensity at a 6-μsec pulse width. For an e^2qQ/h of $\sim$6.5 MHz [CuO_2 planar oxygens O(2,3), or O(1), in $YBa_2Cu_2O_{7-x}$], a maximum in signal intensity would be observed at $1/(I+\frac{1}{2})$ or $\sim$2 μsec, and a second-order contribution to the rotation pattern would be observed, as with $YBa_2Cu_3O_{7-x}$.[29] This observation of a very small e^2qQ/h value for the apical oxygen suggests to us the lack of any large covalent interaction between the oxygens in the La(Sr)O plane with the CuO_2 planar copper atoms.

We have also obtained preliminary results on the (Ba,K)BiO_3 system at 11.7 T and 300 K, and data for $BaBiO_3$, $Ba_{0.8}K_{0.2}BiO_3$, and the superconductor $Ba_{0.6}K_{0.4}BiO_3$ are shown in Fig. 11. Since $BaBiO_3$ contains no magnetic ion, a conventional diamagnetic chemical shift of $\sim$375 ppm from H_2O is found (from a computer line-shape simulation of the second-order powder pattern, for which we find $e^2qQ/h=7.5$ MHz and $\eta=0$). However, upon doping with K^+, we again find a large paramagnetic shift (of $\approx$500 ppm), due in this case perhaps, to the presence of holes on the oxygen sublattice, or in the oxygen p band, consistent with the transformation to the metallic state. Further field- and temperature-dependence studies on this system aimed at analyzing the line-shape and relaxation characteristics of this copper-free system are in progress.

We now try to interpret these results on the superconductors themselves in light of our results on various model compounds.

In the diamagnetic region of the spectrum, we find an interesting apparent correlation between the chemical shifts observed for the superconductors, and those found for some of the "parent" oxides. For example, the SrO plane in $Bi_2Sr_2CaCu_2O_{8+x}$ (197 or 280 ppm) is more shielded than the BaO plane in either $Tl_2Ba_2CaCu_2O_{8+x}$ (either 315 or 350 ppm) or in $YBa_2Cu_2O_{7-x}$ ($\sim$458 ppm), just as SrO itself is considerably more shielded than BaO (Table II). We also find similar trends with the plane 3 sites. Thus Bi_2O_3 ($\delta_i=196$ ppm) is more shielded than Tl_2O_3 ($\delta_i=364$ ppm, Table II), which seems to correlate with the increased shielding found in the BiO plane 3 in $Bi_2Sr_2CaCu_2O_{8+x}$ (197 or 280 ppm) versus the TlO plane 3 in $Tl_2Ba_2CaCu_2O_{8+x}$ (315 or 350 ppm). Although these effects are very small, they may well represent a general trend if magnetic shielding effects from the CuO_2 planes are rather small, since then the large number of nearest-neighbor Ba, Sr, Bi, or Tl atoms in the planes might well have a large influence on δ_i. In any case, our chemical shift results on model compounds indicate that the model systems in general resonate either close to, or a few hundred ppm downfield from, the plane 2 and plane 3 shifts seen in the Cu-containing high-T_c superconductors, in their normal state. This statement applies to each of the La(Sr)O, BaO, SrO, BiO, and TlO sites.

Now, upon cooling into the superconducting state, we showed previously that plane 1 in $YBa_2Cu_3O_{7-x}$ underwent a $\sim$0.1% diamagnetic shift, with the result that the CuO_2 plane site resonated at $\approx$900 ppm, at $\sim$77 K.

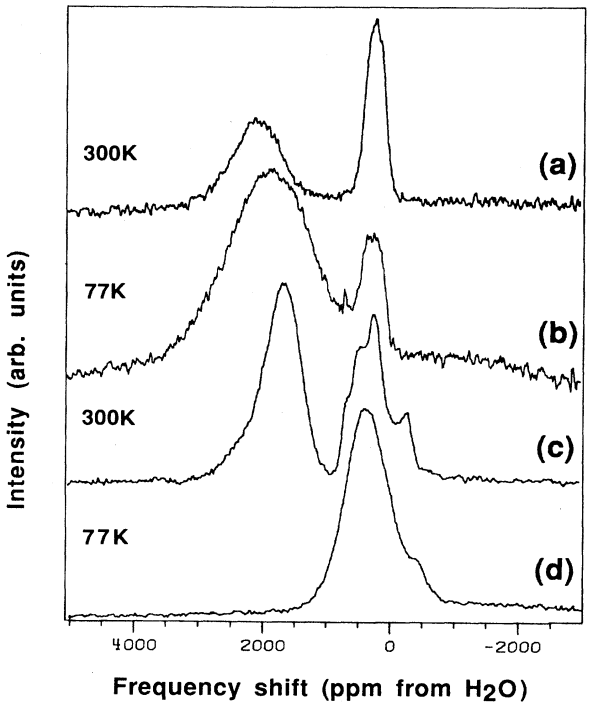

FIG. 12. 8.45-T (48.8-MHz) ^{17}O NMR spectra of (a) $Bi_2Sr_2CaCu_2O_{8+x}$ at 300 K, (b) $Bi_2Sr_2CaCu_2O_{8+x}$ at 77 K, (c) $Tl_2Ba_2CaCu_2O_{8+x}$ at 300 K, (d) $Tl_2Ba_2CaCu_2O_{8+x}$ at 77 K.

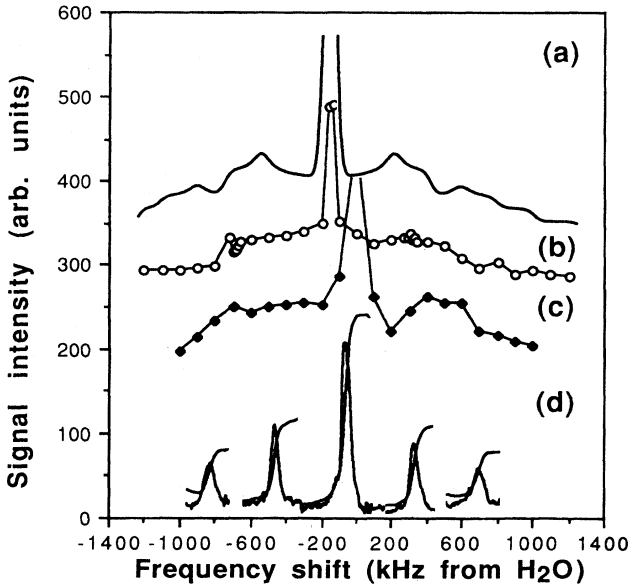

FIG. 13. 8.45-T (48.8-MHz) ^{17}O NMR spectra and computer simulations of high-T_c superconductors. (a) Computer simulation having $\delta_i=1800$ ppm, $e^2qQ/h=6.4$ MHz, $\eta=0.22$. (b) $Bi_2Sr_2CaCu_2O_{8+x}$, 300 K, point-by-point spectrum. (c) $Tl_2Ba_2CaCu_2O_{8+x}$, 77 K, point-by-point spectrum. (d) $YBa_2Cu_3O_{7-x}$, magnetically ordered ($H_0\|c$), 77 K, spectrum taken in five pieces.

We show in Fig. 12 the results of similar experiments on $Bi_2Sr_2CaCu_2O_{8+x}$ and $Tl_2Ba_2CaCu_2O_{8+x}$. For $Bi_2Sr_2CaCu_2O_{8+x}$, the results of Figs. 12(a) and 12(b) indicate only a ~200-ppm diamagnetic shift for plane 1, a result not unexpected since at 8.45 T this material is only beginning to become superconducting, at 77 K. In contrast, the results on $Tl_2Ba_2CaCu_2O_{8+x}$ ($T_c \sim 100$ K) indicate a ~0.13% diamagnetic shift for plane 1, in complete accord with the previous results on $YBa_2Cu_3O_{7-x}$. We believe these results further support our spectral assignments, and again indicate that the CuO_2 planes in both $YBa_2Cu_2O_{7-x}$ and $Tl_2Ba_2CaCu_2O_{8+x}$ have normal "diamagnetic" shifts, of a few hundred ppm from H_2O, in the superconducting state. We note, however, that the diamagnetic shift in $Tl_2Ba_2CaCu_2O_{8+x}$ is a rather monotonic one as a function of temperature, unlike that in $YBa_2Cu_3O_{7-x}$, which could imply a slight oxygen deficiency in this material (as seen in $YBa_2Cu_3O_{6.5}$).

We have also carried out initial experiments to determine e^2qQ/h values for the CuO_2 planar oxygens in $Bi_2Sr_2CaCu_2O_{8+x}$ and $Tl_2Ba_2CaCu_2O_{8+x}$, and our preliminary findings are shown in Fig. 13. Figure 13(a) represents a theoretical line shape for $e^2qQ/h=6.4$ MHz and $\eta=0.2$, close to that found for $YBa_2Cu_3O_{7-x}$. Figure 13(b) shows the point-by-point experimental spin-echo spectra obtained using a fast recycle time (to attenuate signals from planes 2 and 3), for $Bi_2Sr_2CaCu_2O_{8+x}$. There is clearly moderately good agreement between the experimental result and the computer simulation, a result consistent with the finding of Ishida *et al.*[38] Also shown in Fig. 13 are the results we have obtained on $Tl_2Ba_2CaCu_2O_{8+x}$, this time in the superconducting state (at 77 K), Fig. 13(c). Again, there is moderate agreement with the $YBa_2Cu_3O_{7-x}$ simulation, implying $e^2qQ/h \approx 6.4$ MHz. Although additional results are required, the observation of similar CuO_2 plane oxygen e^2qQ/h values in $YBa_2Cu_3O_{7-x}$ and $Bi_2Sr_2CaCu_2O_{8+x}$ at 300 K with that of $Tl_2Ba_2CaCu_2O_{8+x}$ at 77 K ($<T_c$), together with the observation that χ_{zz} for $YBa_2Cu_3O_{7-x}$ also does not change in a major way between 300 K (Fig. 5) and 77 K [Fig. 13(d)], suggests that e^2qQ/h values for the CuO_2 planar oxygens may not change by very much on cooling below T_c.

RELAXATION BEHAVIOR

Over the past few years, we have investigated the ^{17}O NMR behavior of about 50 oxides, mixed oxides, zeolites, polyoxoanions, and (oxo)-macromolecular systems. For almost all *solid* phases, we find from recycle time-dependence studies (which we routinely carry out to determine optimum recycle times) that all T_1 values must be quite long, typically several seconds to tens of seconds, or even longer. This is to be expected for oxygen nuclei in rigid lattice systems. Exceptions are zeolites,[39] where e^2qQ/h is modulated by rapid counterion motions,[40] and in oxypicket-fence-porphyrin, oxymyoglobin, and oxyhemoglobin, where O_2 ligand rotation can reduce T_1.[37] We also find that, in general, spin-echo decays as a function of time ("T_{2e}") are relatively long—since in general

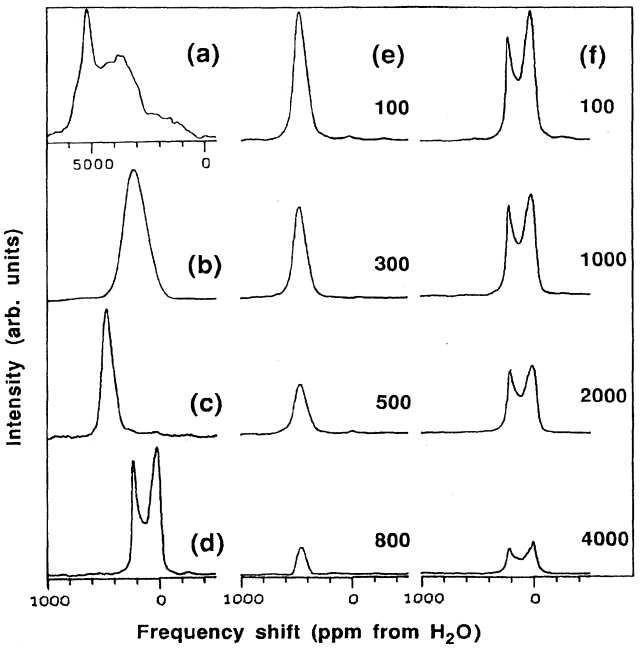

FIG. 14. 11.7-T (67.8-MHz) ^{17}O NMR spectra of selected model compounds, at 300 K; (a) CuO, (b) Bi_2O_3, (c) Tl_2O_3, (d) amorphous SiO_2. (e) Spin-echo decay spectra of Tl_2O_3; the 2τ values shown are in msec. (f) Spin-echo spectra of amorphous SiO_2, the 2τ values shown are in msec.

(inhomogeneous) second-order quadrupole interactions dominate the observed spectral linewidths.[41]

We have now begun a study of T_1 and spin-echo decay ("T_{2e}") relaxation behavior in the high-T_c superconductors, and in a series of model oxides. We show in Fig. 14 typical ^{17}O NMR spectra of CuO [300 K, Fig. 14(a)], Bi_2O_3 [Fig. 14(b)], Tl_2O_3 [Fig. 14(c)], and SiO_2 [Fig. 14(d)]. CuO is a black, antiferromagnetically coupled semiconductor,[42] Bi_2O_3 is a (yellow) semiconductor, Tl_2O_3 is a (black) metallic oxide, and SiO_2 is a conventional (white) diamagnetic insulator. The chemical shifts

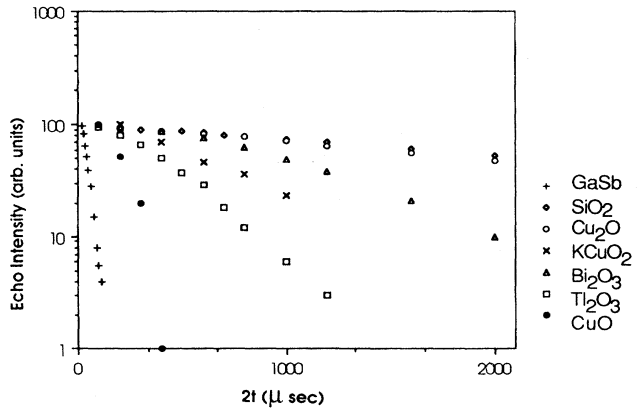

FIG. 15. 11.7-T spin-echo decay results on a variety of model compounds. +, ^{71}Ga NMR in GaSb. ●, ^{17}O NMR in CuO. □, ^{17}O NMR in Tl_2O_3. ×, ^{17}O NMR in $KCuO_2$. △, ^{17}O NMR in Bi_2O_3. ○, ^{17}O NMR in Cu_2O. ◇, ^{17}O NMR in SiO_2.

for Bi_2O_3, Tl_2O_3, and SiO_2 are all in the normal "diamagnetic" chemical shift range alluded to above. Figures 14(e) and 14(f) show the decay of the spin-echo amplitude as a function of delay time (2τ, where τ is the interpulse separation), and represent typical signal-to-noise ratios, and in Fig. 15 we show spin-echo decay measurements on a wide range of model compounds, in graphical form. All decay curves were obtained on polycrystalline materials and show some Gaussian character. For comparison we show, in Fig. 16, results on each of the Cu-containing superconductors (at 300 K), and in Fig. 17 results on $YBa_2Cu_3O_{7-x}$ at 77 K ($< T_c$) as well.

There are a number of interesting features in Figs. 15–17. In Fig. 15, the extremes in T_{2e} behavior are exhibited by GaAs and SiO_2. GaAs has a very rapid T_{2e}, but a T_1 of ~300 msec. The experimentally observed linewidth of ~12 KHz can be accounted for by the overwhelming dominance of spin exchange,[43] and as expected, MASS NMR gives only an insignificant line narrowing.[43]

On the other hand, the spectrum of SiO_2 [Fig. 14(d)] is dominated by the (inhomogeneous) second-order quadrupole interaction, and has a very long T_1 (approximately tens of seconds), with a T_{2e} presumably dominated by homonuclear dipolar interactions.

CuO also has a very rapid decay, again due we believe to exchange coupled interactions. Tl_2O_3 has the next shortest T_{2e}, and the presence of Tl-Tl exchange interactions in this metallic oxide has previously been demonstrated,[44] and exchange interactions in this system might thus also be expected. The Cu(III)-containing species, $KCuO_2$, has a longer T_{2e}, which again likely has an exchange origin, since dipole-dipole interactions are expected to be small—as indicated by the very long T_{2e} result on the Cu^I system Cu_2O (a tan colored semiconductor), as shown in Fig. 15.

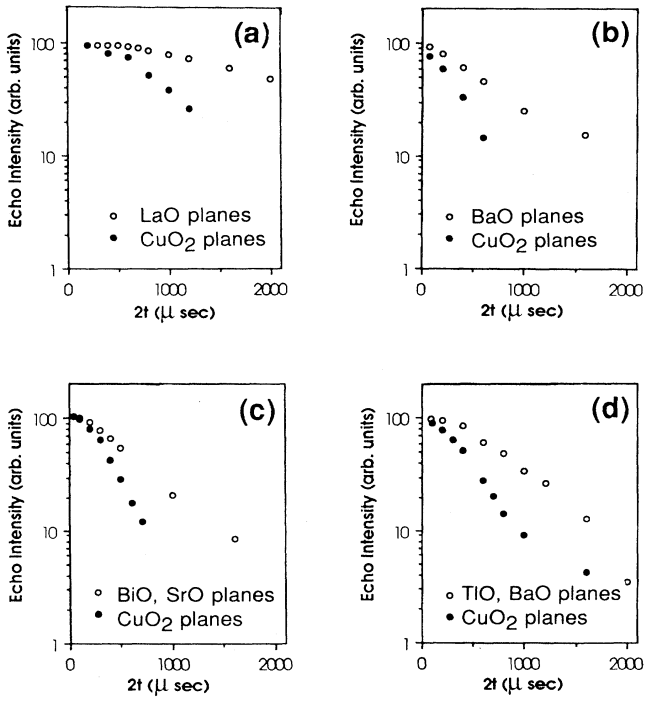

FIG. 16. 11.7-T (67.8-MHz) ^{17}O NMR spin-echo decay behavior at 300 K in (a) $La_{1.85}Sr_{0.15}CuO_4$, (b) $YBa_2Cu_3O_{7-x}$, (c) $Bi_2Sr_2CaCu_2O_{8+x}$, (d) $Tl_2Ba_2CaCu_2O_{8+x}$.

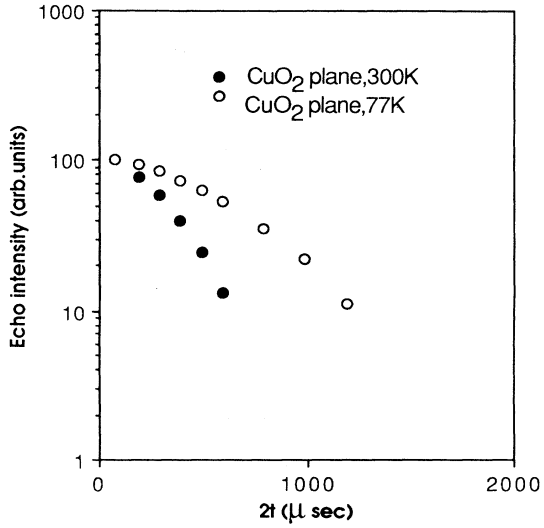

FIG. 17. 8.45-T (48.8-MHz) ^{17}O NMR spin-echo decay behavior at 300 and 77 K in $YBa_2Cu_3O_{7-x}$ (chain and column depleted). ●, CuO_2 plane, 300 K. ○, CuO_2 plane, 77 K ($< T_c$).

The results of Fig. 15 provide a useful data set with which to compare the results obtained on the high-T_c materials (above T_c) shown in Fig. 16. For each of the four main classes of copper-containing superconductor, we show spin-echo decay results for the CuO_2-containing plane 1 (solid circles), and for planes 2 and 3 (open circles). Except for $YBa_2Cu_3O_{7-x}$, we find a much more rapid T_{2e} for the CuO_2 plane sites than for planes 2 and 3 (which have similar behavior). For the Y, Bi, and Tl systems, the echo decays for the CuO_2 planes are longer than for CuO, but are quite close to that of the metallic oxide, Tl_2O_3. Of course, such comparisons are extremely qualitative, but we are primarily interested here in using these relaxation curves to show the great similarities between the four main high-T_c types, since this helps establish our spectral assignments.

For $YBa_2Cu_3O_{7-x}$, we find that the relaxation behavior of the column oxygen [O(1)] is quite anisotropic. We first noticed this effect in the spontaneously self-aligning fraction (* in Figs. 4 and 8), and have confirmed the observation on a highly oriented sample (data not shown). In this system, plane, chain, and column are characterized by fast echo decays ($H_0 \| c$). This behavior appears to correlate with the orientation-dependent linewidth of the apical oxygen in $La_{1.85}Sr_{0.15}CuO_4$.

What is also of some interest is the result we have obtained on $YBa_2Cu_3O_{7-x}$ in the superconducting state (at 77 K), shown in Fig. 17. We find on cooling below T_c that, not only does the CuO_2 plane signal undergo an ~0.1% diamagnetic shift, but the spin-echo decay [for the dominant plane site, O(2,3)] behavior lengthens con-

siderably. A large change in the O-O exchange coupling for O(2,3) below T_c is suggested from this result, correlating presumably with the decreased $(1/T_1)$ behavior observed far below T_c (see below), although the change may not be discontinuous. We are monitoring primarily O(2,3) in this sample, which had been back exchanged with $^{16}O_2$ to remove chain and column contributions to the observed spectrum.

We have also obtained spin-lattice relaxation time (T_1) results on our ^{17}O-labeled materials. We show in Fig. 18 typical recovery curves for $YBa_2Cu_3O_{7-x}$ after a saturating comb, applied on resonance. Results at 300 K for the CuO_2 planar oxygens are similar in an oriented sample and a powder sample, and yield $T_1 \sim 13$ msec. The relaxation time of the column site O(1) (plane 2, bridging oxygen) is considerably longer and slightly anisotropic, the oriented sample had a $T_1 \sim 116$ msec, and the powder a T_1 of ~ 160 msec. In Fig. 19 we show our T_1 results (for a powder sample) on O(1), O(2), and O(3) as a function of temperature, and include for comparison the powder results obtained for O(2,3) by Ishida *et al.*[38] Although Ishida *et al.*[38] imply their sample is labeled solely in the planes, their labeling route would imply uniform labeling (seven rather than four oxygens). However, if fast recycle times were used, then primarily the O(2,3) planar oxygens would be observed. The decreased relaxation rate compared with that we observe may be due to the fact that these authors fitted only the long-time tail of the free induction decay (spin-echo tail), while we have used a triple exponential form of the recovery.[45,46] Indeed, treatment of our data in this manner yields results in much closer agreement with Ishida *et al.*[38] than would be suggested from Fig. 19. Our results are, however, in much better

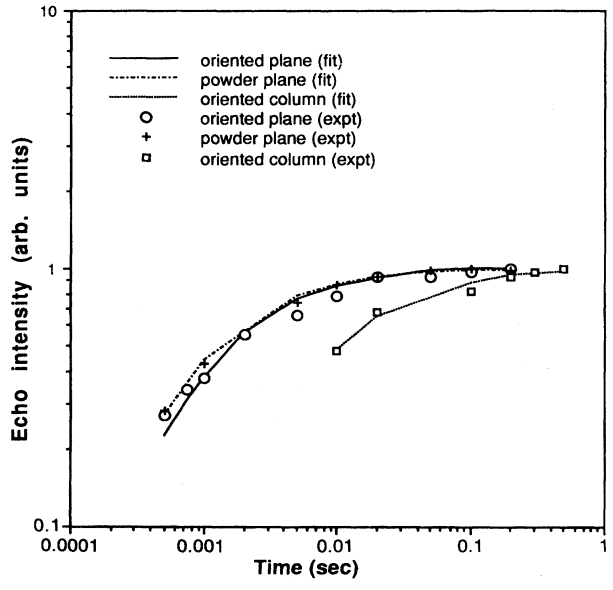

FIG. 18. 8.45-T (48.8-MHz) ^{17}O spin-lattice relaxation data on the oxygen sites of $YBa_2Cu_3O_{7-x}$ for the central transitions, 300 K. The points are the echo intensities, $I(\infty)-I(T)$, measured at time T. A three-exponential recover (magnetic relaxation mechanism) was used to fit each data set.

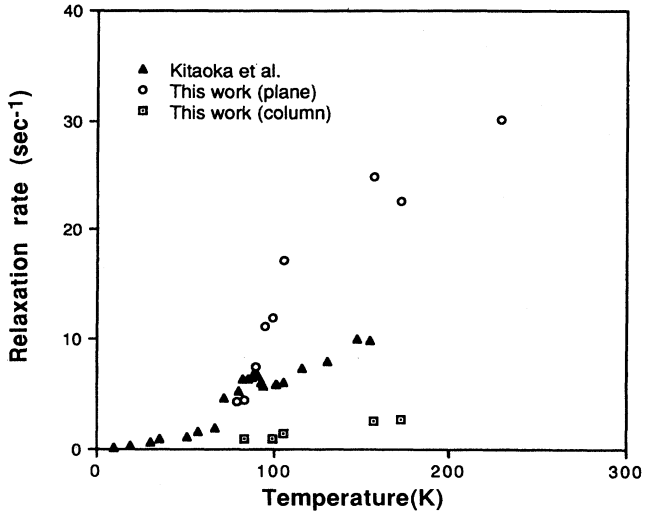

FIG. 19. Relaxation rates as a function of temperature for $YBa_2Cu_3O_{7-x}$ powder as reported by Ishida *et al.* (Ref. 38) for the plane site (▲) and in this work for the plane (○) and bridging oxygen sites. Data obtained on a random powder sample, on resonance.

agreement with those of Hammel[36] on oriented samples, our T_1 values being about a factor of 2 slower.

For all three groups, the T_1 results indicate Korringa-type behavior above T_c, in sharp contrast to the Cu NMR results on Cu(2).[47] Using the following form of the Korringa relaxation expression:

$$T_1 = \frac{\hbar}{4\pi kT}\left[\frac{\gamma_e}{\gamma_n}\right]^2\left[\frac{H}{\Delta H}\right]^2 \tag{14}$$

we can estimate the T_1 values expected, from the observed shifts. A lower estimate on the Knight shift can be obtained from a measure of the diamagnetic shifts observed on cooling $YBa_2Cu_3O_{7-x}$ and $Tl_2Ba_2CaCu_2O_{8+x}$ to 77 K. For $YBa_2Cu_3O_{7-x}$ we find $K \sim 0.11\%$, and for $Tl_2Ba_2CaCu_2O_{8+x}$, $K \sim 0.13\%$. A 0.12% shift would predict a T_1 at 100 K of ~ 100 msec or $1/T_1 \sim 10$ sec^{-1}. However, it seems unlikely that the superconducting transitions at 8.45 T are complete at 77 K for either system, and perhaps a more reasonable diamagnetic shift of ^{17}O would be in the range -181 ppm (Cu_2O) to ~ 30 ppm ($KCuO_2$). Using an average of these values yields $K \approx 0.19\%$, for which $1/T_1 \sim 26$ sec^{-1}. Our determined $1/T_1$ of ~ 18 sec^{-1} at 100 K clearly falls within the range 10–26 sec^{-1} (at 100 K), and, consistent with the experimentally determined Korringa behavior above T_c observed by all groups, supports the origin of the large ^{17}O NMR shifts of the plane oxygens as a Knight shift. Thus oxygens in the CuO_2 planes in $YBa_2Cu_3O_{7-x}$, $Bi_2Sr_2CaCu_2O_{8+x}$, and $Tl_2Ba_2CaCu_2O_{8+x}$ are all, more likely than not, shifted by a Knight shift interaction, based on our ^{17}O NMR T_1 (see below) and frequency-shift behavior, and each of these planes can thus be described as being metallic. These results are in sharp contrast to the Cu NMR data, which do not show Korringa

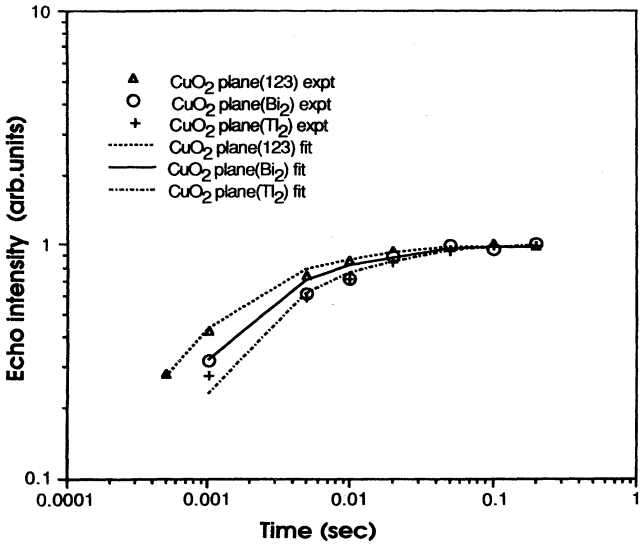

FIG. 20. ^{17}O NMR spin-lattice relaxation data at 300 K for the CuO_2 central transition of the planar sites for $YBa_2Cu_3O_{7-x}$ (48.8 MHz), $Bi_2Sr_2CaCu_2O_{8+x}$ (67.8 MHz), and $Tl_2Ba_2CaCu_2O_{8+x}$ (67.8 MHz). The points are the echo intensities $I(\infty)-I(T)$ measured at a time T after a long comb of pulses. The lines are the theoretical fits to the data.

behavior, and have been attributed to antiferromagnetic spin fluctuations,[47] with localized moments on Cu(2).[48,49]

Below T_c, although we have only a very limited data set at present, our relaxation rate results again suggest for the planar oxygens a power-law behavior, similar to the behavior seen for Cu(2) NMR by several groups, and as observed by Hammel for O(2,3).[36] Our results show no evidence for a BCS-type enhancement in $1/T_1$ just below T_c. However, as Koyama and Tachiki have noted,[50] spin fluctuation could make the superconducting state gapless at T_c, resulting in power-law behavior below T_c with no BCS enhancement.

For the column oxygen, O(1), our relaxation rate results show a power-law temperature dependence greater than linear just as observed by Hammel for the chain site [O(4)].[36] As noted by Hammel, the chain relaxation rate $(1/T_1)$ above T_c closely resembles that of the Cu(1) NMR, and our results suggest a similar effect for the column site, O(1) [both O(1) and O(4) are bound to Cu(1)].

Finally, we show in Fig. 20 experimental saturating comb-recovery results on the CuO_2 planar sites in $YBa_2Cu_3O_{7-x}$, $Bi_2Sr_2CaCu_2O_{8+x}$, and $Tl_2Ba_2CaCu_2O_{8+x}$, at 300 K. We find T_1 values of ~ 13, ~ 21, and ~ 32 msec, respectively. These results were all obtained on resonance on powder samples using a three-exponential recovery fit to the data, as shown in Fig. 20. Taken together with the shift and echo decay results presented above, we believe there is a remarkable similarity between all three superconductors, and we believe a reasonable prediction, based on the T_1, echo decay, and frequency-shift results, is that all three show metallic, Korringa-type relaxation behavior in their normal state. With $YBa_2Cu_3O_{7-x}$, the enhanced $1/T_1$ at 300 K implies additional relaxation pathways at this temperature. Further studies of this effect, which should be dependent on the details of sample preparation, are in progress. We also note, as can be deduced from the results shown in Fig. 12, that T_1 values found for the BaO, SrO, BiO, and TlO planes in all materials are much longer than those for the CuO planes. This observation is consistent with their normal state diamagnetic shifts and the lack of any large frequency shifts for planes 2 and 3 upon cooling to 77 K. Spin contributions to the frequency shift for these sites thus appear to be relatively small.

CONCLUSIONS

We believe our results are of interest for several reasons. First, we have been able to obtain resolved ^{17}O NMR spectra for most of the main types of high-T_c superconductor. We find in general that the ^{17}O NMR spectra of each copper-containing system contain a highly paramagnetically shifted resonance, due to the CuO_2 planes, and a feature or series of features in a much more diamagnetically shifted region, attributable to the non-copper-containing planar sites. The CuO_2 planar oxygens undergo a large diamagnetic shift (in $YBa_2Cu_3O_{7-x}$ and $Tl_2Ba_2CaCu_2O_{8+x}$) on cooling to 77 K. For this feature in $YBa_2Cu_3O_{7-x}$, T_1 relaxation measurements as a function of temperature, above T_c, indicate Korringa-type (metallic) relaxation behavior, and the estimated Knight sift is in reasonable accord with the actual shift observed. There seems to be no large change in e^2qQ/h of the planar oxygens on cooling below T_c. The T_1 values for the CuO_2 sites in the Y, Bi, and Tl materials are all quite similar. T_2 relaxation (or spin-echo decay behavior) in powder samples for the CuO_2 planar sites (in $La_{0.85}Sr_{0.15}CuO_4$, $YBa_2Cu_3O_{7-x}$, $Bi_2Sr_2CaCu_2O_{8+x}$, and $Tl_2Ba_2CaCu_2O_{8+x}$) is much more rapid than for the non-CuO_2 planar sites, and suggests a magnetic exchange origin. This effect seems to be decreased in the superconducting state (for $YBa_2Cu_3O_{7-x}$, at 77 K). The Cu-free system also exhibits a large paramagnetic shift (on K^+ doping), on formation of the metallic state.

ACKNOWLEDGMENTS

We are grateful to Professor C. P. Slichter, for his continuous flow of advice, and for copies of his work prior to publication; to Professor T. B. Rauchfuss, for invaluable help with the synthetic work; to Professor R. M. Martin, for his valuable advice; to Dr. P. C. Hammel, for generously providing us with copies of his ^{17}O NMR work prior to publication; to Dr. N. Janes, for helpful comments; to Dr. G. L. Turner and S. E. Chung, for provision of ^{17}O chemical shift results on some model compounds; and to Bernard Montez, for help with data acquisition and instrumentation. This work was supported in part by the Solid State Chemistry Program of the National Science Foundation (Grants No. DMR 86-15206 and 88-14789) and by the Materials Research Laboratory Program (Grant No. DMR 86-12860).

[1]J. F. Schooley, W. R. Hosler, and M. Cohen, Phys. Rev. Lett. **12**, 474 (1964).
[2]J. P. Remeika, T. H. Geballe, B. T. Matthias, A. S. Cooper, G. W. Hull, and E. M. Kelly, Phys. Lett. **24A**, 565 (1967); D. R. Wanlass and M. J. Sienko, J. Solid State Chem. **12**, 362 (1975).
[3]A. W. Sleight, J. L. Gillson, and P. E. Bierstedt, Solid State Commun. **17**, 27 (1975).
[4]J. G. Bednorz and K. A. Müller, Z. Phys. B **64**, 189 (1986).
[5]M. K. Wu, J. R. Ashburn, C. J. Torng, P. H. Hor, R. L. Meng, L. Gao, Z. J. Huang, Y. Q. Wang, and C. W. Chu, Phys. Rev. Lett. **58**, 908 (1987); P. H. Hor, L. Gao, R. L. Meng, Z. J. Huang, Y. Q. Wang, K. Forster, J. Vassilious, C. W. Chu, M. K. Wu, J. R. Ashburn, and C. J. Jorng, *ibid.* **58**, 911 (1987).
[6]Y. LePage, W. R. McKinnon, J. M. Tarascon, L. H. Greene, G. W. Hull, and D. M. Huwang, Phys. Rev. B **35**, 7245 (1987); J. M. Tarascon, P. Barboux, B. G. Bagley, L. H. Greene, W. R. McKinnon, and G. W. Hull, ACS Symp. Ser. **351**, 198 (1987).
[7]T. Siegrist, S. Sunshine, D. W. Murphy, R. J. Cava, and S. M. Zahurak, Phys. Rev. B **35**, 7137 (1987).
[8]M. A. Subramanian, C. C. Torardi, J. C. Calabrese, J. Gopalakrishnan, K. J. Morrissey, T. R. Askew, R. B. Flippen, U. Chowdhry, and A. W. Sleight, Science **239**, 1015 (1988).
[9]H. Maeda, Y. Tanaka, M. Fukutomi, and T. Asano, Jpn. J. Appl. Phys. **27**, L209 (1988); M. Onoda, A. Yamamoto, E. Takayama-Muromachi, and S. Takekawa, *ibid.* **27**, L833 (1988).
[10]Z. Z. Sheng and A. M. Hermann, Nature (London) **332**, 55 (1988); **332**, 138 (1988); Y. Shimakawa, Y. Kubo, T. Manako, Y. Nakabayashi, and H. Igarashi, Physica B+C **156C**, 97 (1988).
[11]L. C. Hebel and C. P. Slichter, Phys. Rev. **113**, 1504 (1959).
[12]J. Bardeen, L. N. Cooper, and J. R. Schrieffer, Phys. Rev. **108**, 1175 (1957).
[13]M. Lee, M. Yudkowsky, W. P. Halperin, J. Thiel, S.-J. Hwu, and K. R. Poeppelmeier, Phys. Rev. B **36**, 2378 (1987).
[14]R. E. Walstedt, W. W. Warren, Jr., R. F. Bell, G. F. Brennert, G. P. Espinosa, J. P. Reimeika, R. J. Cava, and E. A. Reitman, Phys. Rev. B **36**, 5727 (1987).
[15]Z. Furo, A. Jánossy, L. Milhály, P. Bánki, I. Pócsik, I. Bakonyi, I. Heinmaa, E. Joon, and E. Lippmaa, Phys. Rev. B **36**, 5690 (1987).
[16]C. H. Pennington, D. J. Durand, D. B. Zax, C. P. Slichter, J. P. Rice, and D. M. Ginsberg, Phys. Rev. B **37**, 7944 (1988).
[17]J. T. Markert, T. W. Noh, S. E. Russek, and R. M. Cotts, Solid State Commun. **63**, 847 (1987).
[18]G. J. Kramer, H. B. Brom, J. van den Berg, P. H. Kes, and D. J. W. Ijdo, Solid State Commun. **64**, 705 (1987).
[19]H. B. Brom, G. J. Kramer, J. van den Berg, and J. C. Jol, Phys. Rev. B **38**, 2886 (1988).
[20]P. Butaud, P. Ségransan, C. Berthier, Y. Berthier, C. Paulsen, J. L. Tholence, and P. Lejay, Phys. Rev. B **36**, 5702 (1987).
[21]H. Lütgemeir and M. W. Pieper, Solid State Commun. **64**, 267 (1987).
[22]N. Janes and E. Oldfield, J. Am. Chem. Soc. **108**, 5743 (1986).
[23]G. L. Turner, S. E. Chung, and E. Oldfield, J. Magn. Res. **64**, 316 (1985).
[24]S. Yang, K. D. Park, and E. Oldfield (unpublished).
[25]S. Schramm and E. Oldfield, J. Am. Chem. Soc. **106**, 2502 (1984).
[26]H. K. C. Timken, N. Janes, G. L. Turner, S. L. Lambert, L. B. Welsh, and E. Oldfield, J. Am. Chem. Soc. **108**, 7236 (1986).
[27]A. Nayeem and J. P. Yesinowski, J. Chem. Phys. **89**, 4600 (1988).
[28]A. C. Kunwar, G. L. Turner, and E. Oldfield, J. Magn. Res. **69**, 124 (1986).
[29]C. Coretsopoulos, H. C. Lee, E. Ramli, L. Reven, T. B. Rauchfuss, and E. Oldfield, Phys. Rev. B **39**, 781 (1989).
[30]D. E. Farrell, B. S. Chandrasekhar, M. R. DeGuire, M. M. Fang, V. G. Kogan, J. R. Clem, and D. K. Finnemore, Phys. Rev. B **36**, 4025 (1987).
[31]D. U. Gubser, R. A. Hein, S. H. Lawrence, M. S. Osofsky, D. J. Schrodt, L. E. Toth, and S. A. Wolf, Phys. Rev. B **35**, 5350 (1987).
[32]D. G. Hinks, B. Dabrowski, J. D. Jorgensen, A. W. Mitchell, D. R. Richards, S. Pei, and D. Shi, Nature (London) **333**, 836 (1988).
[33]K. C. Ott *et al.*, Phys. Rev. B **39**, 4285 (1989).
[34]P. S. Kobiela, D. Sun, C. B. Prater, W. P. Kirk, and D. G. Naugle (unpublished).
[35]H. Bleier, P. Bernier, D. Jérome, J. M. Bassat, J. P. Coutures, B. Dubois, and Ph. Odier, J. Phys. (Paris) **49**, 1825 (1988).
[36]P. C. Hammel (private communication).
[37]K. B. Lyons, P. A. Fleury, L. F. Schneemeyer, and J. V. Waszczak, Phys. Rev. Lett. **60**, 732 (1988).
[38]K. Ishida, Y. Kitaoka, K. Asayama, H. Katayama-Shida, Y. Okabe, and T. Takahashi, J. Phys. Soc. Jpn. **57**, 2897 (1988).
[39]H. K. C. Timken, Ph.D. thesis, University of Illinois, 1986 (unpublished).
[40]J. Haase, H. Pfeiffer, W. Oehme, and J. Klinowski, Chem. Phys. Lett. **150**, 189 (1988).
[41]H. C. Lee, C. Coretsopoulos, and E. Oldfield (unpublished).
[42]B. X. Yang, J. M. Tranquada, and G. Shirane, Phys. Rev. B **38**, 174 (1988).
[43]O. H. Han, H. K. C. Timken, and E. Oldfield, J. Chem. Phys. **89**, 6046 (1988).
[44]N. Bloembergen and T. J. Rowland, Phys. Rev. **97**, 1679 (1955).
[45]E. R. Andrew and D. P. Tunstall, Proc. Phys. Soc. London **78**, 1 (1961).
[46]W. W. Simmons, W. J. O'Sullivan, and W. A. Robinson, Phys. Rev. **127**, 1168 (1962).
[47]Y. Kitaoka, S. Hiramatsu, T. Kondon, and K. Asayama, J. Phys. Soc. Jpn. **57**, 30 (1988).
[48]C. H. Pennington, D. J. Durand, C. P. Slichter, J. P. Rice, E. D. Bukowski, and D. M. Ginsberg, Phys. Rev. B **39**, 274 (1989).
[49]C. H. Pennington, D. J. Durand, C. P. Slichter, J. P. Rice, E. D. Bukowski, and D. M. Ginsberg, Phys. Rev. B **39**, 2902 (1989).
[50]T. Koyama and M. Tachiki, Phys. Rev. B **39**, 2279 (1989).